Synthesis, characterization and biological activity of new cyclometallated platinum(IV) iodide complexes†

Emma Bauer,[a] Xavier Domingo,[a] Cristina Balcells, [b,c] Ibrahim H. Polat,[b,c] Margarita Crespo, [*a,c] Josefina Quirante, [*c,d] Josefa Badía, [c,e,] Laura Baldomà, [c,e], Mercè Font-Bardia [f] and Marta Cascante [b,c]

aDepartament de Química Inorgànica i Orgànica, Secció de Química Inorgànica, Facultat de Química, Universitat de Barcelona, Diagonal 645, 08028-Barcelona, Spain. E-mail: margarita.crespo@qi.ub.es

bDepartment of Biochemistry and Molecular Biomedicine, Faculty of Biology, Universitat de Barcelona, Av. Diagonal 643, 08028-Barcelona, Spain

cInstitut de Biomedicina de la Universitat de Barcelona (IBUB), Av. Diagonal 643, 08028-Barcelona, Spain

dLaboratori de Química Orgànica, Facultat de Farmàcia, Universitat de Barcelona, Av. Joan XXIII, 27-31, 08028-Barcelona, Spain. E-mail: quirantese@ub.edu

eDepartament de Bioquímica i Fisiologia, Secció de Bioquímica i Biologia Molecular, Facultat de Farmàcia, Av. Joan XXIII, 27-31, 08028-Barcelona, Spain

fUnitat de Difracció de RX, Centres Científics i Tecnològics de la Universitat de Barcelona (CCiTUB), Universitat de Barcelona, Solé i Sabarís 1-3, 08028-Barcelona, Spain

.

ABSTRACT:

The synthesis of six novel cyclometallated platinum(IV) iodido complexes is accomplished by intermolecular oxidative addition of methyl iodide (compounds 2a–2c) or iodine (compounds 3a–3c) upon cyclometallated platinum(II) compounds [PtX{(CH3)2N(CH2)3NCH(4-ClC6H3)}] (1a–1c: X = Cl, CH3 or I). The X-ray molecular structures of platinum(II) compound 1c and platinum(IV) compounds 3b and 3a' (an isomer of 3a) are reported. The cytotoxic activity against a panel of human adenocarcinoma cell lines (A-549 lung, MDA-MB-231 and MCF-7 breast, and HCT-116 colon), DNA interaction, topoisomerase I, IIα, and cathepsin B inhibition, and cell cycle arrest, apoptosis and ROS generation of the investigated complexes are presented. Remarkable antiproliferative activity was observed for most of the synthesized cycloplatinated compounds (series 1–3) in all the selected carcinoma cell lines. The best inhibition was provided for the octahedral platinum(IV) compounds 2a–2c exhibiting a methyl and an iodido axial ligand. Preliminary biological results point to a different mechanism of action for the investigated compounds. Cyclometallated platinum(II) compounds 1a–1c modify the DNA migration as cisplatin. In contrast, cyclometallated platinum(IV) compounds 2a–2c and 3a–3c did not modify the DNA tertiary structure neither in the absence nor in the presence of ascorbic acid, which made them incapable of reducing platinum(IV) compounds 2b and 2c in a buffered aqueous medium (pH 7.40) according to 1H NMR experiments. Remarkable topoisomerase IIα inhibitory activity is reported for platinum(IV) complexes 2b and 3a and in addition, for the last one, a moderate cathepsin B inhibition is reported. Cell cycle arrest (decrease in G0/G1 and G2 phases and arrest in the S phase), induction of apoptosis and ROS generation are related to the antiproliferative activity of some representative octahedral cyclometallated platinum(IV) compounds (2band 2c).

INTRODUCTION

Following the well-established square-planar platinum(II) anticancer drugs, octahedral platinum(IV) complexes currently attract a great deal of attention as they display a number of advantages related to their inertness and to the possibility of tuning their properties through the additional axial ligands.1–4 Although several platinum(IV) complexes have undergone clinical trials, none has been approved to date, and the rational design of new platinum(IV) potential antitumor agents still remains a challenge. On the other hand, in the last few years, the antitumor properties of cyclometallated platinum(II) compounds have been studied by several groups5–12 including ours.13–16 These compounds present several advantages such as high stability and increased lability of the leaving groups due to the strong transeffect of C-donor ligands. Surprisingly, very little attention has been devoted to cyclometallated platinum(IV) compounds16,17 although these species combine the properties imparted by the presence of a platinum(IV) center and a cyclometallated ligand.

Cyclometallated platinum(IV) compounds can be obtained in a straightforward process consisting of intramolecular C–X bond activation from an adequate platinum(II) substrate and a potentially tridentate [C,N,N′] ligand (method A in Scheme 1).16,18–22 Alternatively, these compounds can be obtained in a two-step process in which the previous synthesis of cyclometallated platinum(II) compounds is followed by intermolecular oxidative addition (method B in Scheme 1). The second route presents some advantages since it allows the synthesis of cyclometallated platinum(IV) compounds with either identical or distinct axial ligands as well as a direct comparison of the properties of the platinum(IV) compounds with those of the parent cyclometallated platinum(II) compound. Moreover, in these compounds, the nature of the axial ligands Y, Z and that of the equatorial ligand X (see Scheme 1) can be easily modified.

Intermolecular oxidative addition has been extensively studied on square-planar platinum(II) compounds and it is generally observed that the set of equatorial ligands of the resulting platinum(IV) compounds retain the stereochemistry of the starting platinum(II) compound while the new ligands occupy the axial positions.23,24 Intermolecular oxidative addition on coordination compounds such as cisplatin, carboplatin and their analogues is often the method of choice to prepare platinum(IV) prodrugs with the most widely used oxidizing agents being halogens or hydrogen peroxide.25–31

Oxidative addition reactions on cyclometallated platinum(II) compounds have received less attention and often involve reagents such as methyl iodide.32–35 In this work, the oxidative addition of both methyl iodide and iodine to several cyclometallated platinum(II) compounds was studied with the purpose of developing a systematic method to prepare novel octahedral cyclometallated platinum(IV) compounds potentially useful as antitumor agents.

.

RESULTS AND DISCUSSION

Syntheses and characterization

Three [C,N,N′] cyclometallated platinum(II) compounds of the general formula [PtX{(CH3)2N(CH2)3NCH(4-ClC6H3)}] (1a–1c) were prepared from imine (CH3)2N(CH2)3NCH(4-ClC6H3) and adequate platinum precursors (see Scheme 2). The synthesis of compound 1a (X = Cl) from cis-[PtCl2(dmso)2] and the molecular structure of 1a have been previously reported.36 Compound 1b (X = CH3) was prepared from [Pt2(CH3)4{μ-S (CH3)2}2] following previously reported procedures for analogous compounds.19,37 Interest in compounds containing a methyl ligand arises from the fact that additional C-donor ligands might further increase both the stability of the compound and the lability of the ligand in trans. In addition, in view of the renewed interest in iodinated platinum(II) complexes as antitumor agents,38–40 platinum(II) compound 1c containing an iodido ligand was also prepared in this work. This compound was initially obtained from the reaction of 1a with AgNO3, followed by a reaction with potassium iodide. However, better yields and purity were achieved using cis-[PtI2(dmso)2]41 as a metallating agent, reaction conditions similar to those previously described for the synthesis of 1a36 and a reaction time of 48 hours. The structure of compound 1c was determined crystallographically and is shown in Fig. 1. As expected,19,36,37 the metallacycle adopts a practically planar arrangement and is nearly coplanar with the coordination plane, the dihedral angle between the mean planes being 4.02°. Although the chelate six-membered ring deviates from planarity, the mean plane of the (N,N′) chelate is only tilted 7.17° from the coordination plane. Most bond angles at platinum are close to the ideal value of 90°, and the smallest angle (80.64°) corresponds to the metallacycle. A comparison of the bond distances with those of 1a reveals that the presence of an iodido instead of a chlorido ligand shortens the Pt–Nimine bond in trans while the bond distances in cis (Pt–N(CH3)2 and Pt–C) are elongated.

In addition, the new cyclometallated platinum(II) compounds 1b and 1c were characterized by NMR spectroscopy. For both compounds, N(CH3)2 appears as a singlet integrating for 6H and coupled to platinum and the imine proton is also coupled to platinum. The 3J (Pt–H) values (59.6 Hz for 1b and 139.0 Hz for 1c) are consistent with the presence of a methyl or an iodido ligand in trans, respectively. In addition, the aromatic proton Ha is also coupled to 195Pt (3J (Pt–H) = 65.2 Hz for 1b and 48.6 Hz for 1c) and is down-field shifted for 1c when compared to 1b (8.75 vs. 7.63 ppm).

Oxidative addition reactions with methyl iodide and iodine were carried out on compounds 1a–1c in order to produce octahedral cyclometallated platinum(IV) compounds containing either two distinct (2a–2c) or two identical (3a–3c) ligands in the axial positions (see Scheme 1). The proposed mechanisms for both methyl iodide24 and iodine42 oxidative addition reactions point to the formation of octahedral platinum(IV) compounds in which the new ligands are mutually trans as depicted in Scheme 3. Nevertheless, further isomerization reactions might bring these ligands to mutually cis positions.

Compound 1b containing an electron-donating methyl ligand is expected to react more readily in these reactions. In fact, the oxidative addition reactions took place in all cases but it was observed that while the reaction of 1b with CH3I is completed in one hour, 1a and 1c require longer reaction times. The obtained compounds 2a–2c were characterized by 1H NMR spectra in which the N(CH3)2 and the (CH2)3 protons are diastereotopic due to the absence of a symmetry plane. In contrast, compounds 3a–3c obtained in the reactions with iodine display simpler 1H NMR spectra due to the equivalence of the dimethylamino and the methylene protons. Selected 1H NMR data of platinum(IV) compounds 2a–2c and 3a–3c are collected in Table 1 along with those obtained for the parent platinum(II) compounds 1a–1c.

The expected reduction of J (Pt–H) values upon oxidation18,19,43 is observed for the imine proton when platinum(IV) compounds are compared with the corresponding parent platinum(II) precursor (2a and 3a vs.1a, 2b and 3b vs. 1b, 2c and 3c vs. 1c) and as indicated for platinum(II) compounds, the value of this coupling constant strongly depends on the nature of the group in trans to the imine. The values of 2J (Pt–H) for the methyl ligand also decrease upon oxidation of the platinum,19 for instance 2J (Pt–H) = 80.8 Hz for 1b decreases to 69.2 Hz upon oxidative addition of iodine (3b). It is interesting to point out that compounds 2c and 3b are geometric isomers with the methyl ligand, either trans to the iodido ligand (2c) or to the imine group (3b). The methyl-platinum protons of these isomers are observed at distinct chemical shift values (1.71 (2c) vs. 2.21 ppm (3b)) while only a small difference in the 2J (Pt–H) values is observed (65.5 vs. 69.2 Hz, respectively). Similar 2J (Pt–H) values are obtained for 2b which contains two methyl ligands, the equatorial trans to an imine and the axial trans to an iodido ligand. In addition, compound 3b was characterized crystallographically (see below).

While compounds 2a, 2c, 3b and 3c are obtained as a single isomer according to the obtained NMR spectra, a careful inspection of the 1H NMR spectra of the cyclometallated platinum(IV) compounds 2b and 3a reveals the presence of a minor isomer in an amount of less than 10% of the mixture. The isomerization of compound 3a could arise from the exchange of the positions of the chlorido and the iodide ligands leading to 3a′ depicted in Scheme 4. This is consistent with the fact that compound 3c, containing only iodide ligands, does not show isomerization. In addition, upon crystallization of 3a in dichloromethane–methanol mixtures, crystals of 3a′ were obtained as deduced from crystallographic analyses (see below). In contrast, the presence of a minor isomer of 2b should be assigned to the I/N(CH3)2 exchange leading to compound 2b″, since the three C-donor ligands always adopt a fac-PtC3 arrangement in octahedral platinum(IV) compounds. 17,19,20 This type of mer- to fac-[C,N,N′] isomerization has been described for analogous cyclometallated platinum(IV) compounds containing three C-donor ligands.19,20

The structures of 3b and 3a′ were determined crystallographically and are shown in Fig. 2 and 3, respectively. For 3b, two independent molecules with bond parameters equal within the experimental error [3σ] are present in the asymmetric unit. As expected from NMR studies, for both 3b and 3a′, the platinum atom displays an octahedral coordination with a meridional tridentate [C,N,N′] ligand. An

equatorial methyl and two axial iodido ligands (3b) or an axial chloride and two mutually cis iodido ligands (3a′) complete the coordination around the platinum. The main distortion from the ideal octahedral coordination is due to the small bite angle of the metallacycles (3b, 79.76(8)° and 3a′, 80.5(3)°). In both cases, the metallacycle is planar and nearly coplanar with both the coordination plane and the mean plane of the (N,N′) chelate. For 3b, the axial ligands form an I–Pt–I angle of 170.128(6)°, somewhat smaller than that reported for the platinum(IV) prodrug of cisplatin cis,cis,trans-[Pt(NH3)2Cl2I2].25 A comparison of the bond distances with those of 1c reveals that the equatorial Pt–Nimine, Pt–N(CH3)2 and Pt–C bond lengths are moderately longer for the platinum(IV) compounds 3b and 3a′. In addition, the Pt–Nimine bond is longer for 3b (trans to the methyl ligand) than for 3a′ (trans to the iodido ligand) in agreement with the higher trans influence of C-donor ligands.

Solution studies: stability and reduction behavior with ascorbic acid

The stability of platinum(IV) compounds 2b and 2c in the aqueous biological media was evaluated by recording the 1H NMR spectra of the compounds (1 mM) in 50 mM phosphate buffer (in D2O, pD 7.40); 2 drops of deuterated DMSO were added to solubilize the compound in the media. The obtained spectra, shown in the ESI (Fig. S1 and S2†), were compared with those obtained at different storage periods. For 2b, from the very beginning until the last recorded spectrum after 10 days, the same product is observed. This compound displays an imine resonance at 8.59 ppm coupled to 195Pt (3J(H–Pt) = 52 Hz) and two methyl resonances coupled to platinum at 0.65 ppm (2J(H–Pt) = 80 Hz) and 0.92 ppm (2J(H–Pt) = 64 Hz) assigned to the axial and equatorial methyl ligands, respectively. These results are consistent with a fast substitution of the axial iodido ligand (trans to the axial methyl ligand) in compound 2b by water or dimethylsulfoxide in agreement with the high trans influence of the carbon atom. The newly formed solvated species (Ib) is stable after 10 days without any evidence of decomposition (Fig. S1 in the ESI†). For 2c, two products showed up from the very beginning and the relative intensities of the signals changed along the monitored period (Fig. S2 in the ESI†). This result suggests that in this case substitution of both iodido ligands for the solvent might take place sequentially leading to species Ic and II as shown in Scheme 5. The substitution is faster for the iodido in trans to the methyl group than for the iodido in trans to the nitrogen atom and the proportion of solvated species II increases with time while that of species Ic decreases. The replacement of the N(CH3)2 moiety of the [C,N,N′] ligand by either D2O or d6- DMSO leading to species III cannot be ruled out since platinum satellites could not be observed clearly for this signal.

The reaction with ascorbic acid, a biologically relevant reducing agent, was monitored by 1H NMR spectroscopy using analogous conditions [1 mM of platinum(IV) compound + 2 drops of deuterated DMSO + 50 mM phosphate buffer and 25 Mm ascorbic acid] and the obtained spectra are given in the ESI (Fig. S3 and S4†). Again, for compounds 2b and 2c, the aromatic and imine regions were most informative since in these regions neither the solvents nor the ascorbic acid interfere with the signals of complexes 2b and 2c. No evidence was found for the reduction of the platinum(IV) complexes 2b and

2c to the corresponding reduced platinum(II) compounds 1b and 1c. For 2b, the initially formed species is stable after ten days as evidenced by the lack of changes in the aromatic and imine regions (Fig. S3 in the ESI†). The two methylplatinum resonances at 0.45 ppm (2J(H–Pt) = 56 Hz) and 0.92 ppm (2J(H–Pt) = 64 Hz) also remain unchanged after ten days. A comparison of these values with those observed for species Ib indicated that the axial methyl signal is shifted from 0.65 ppm (2J(H–Pt) = 80 Hz) to 0.45 ppm (2J(H–Pt) = 56 Hz) and this suggests that the solvent coordinated in trans to the axial methyl in Ib could be replaced by ascorbic acid, leading to species IV. For 2c, a new species that remains stable after 72 h is formed upon adding the ascorbic acid (Fig. S4 in the ESI†). Since compound 2c displays two labile Pt–I bonds, the coordination of ascorbic acid in both positions, either as two monodentate or one bidentate ligand as shown in species V, is possible. In this case, a comparison of the obtained NMR data with those of Ic suggests that a change of both the axial and the equatorial ligands should affect more the chemical shift of the aromatic and imine signals of the final product than when exclusively the axial ligand is changed as for species IV.

BIOLOGICAL STUDIES

Antiproliferative assay

The antiproliferative activity of cyclometallated Pt(II) (1a–1c)and cyclometallated Pt(IV) (2a–2c and 3a–3c) complexes along with cisplatin, as a positive control, was determined by using the MTT assay. The non-small A-549 lung, HCT-116 colon and MCF-7 and MDA-MB-231 breast adenocarcinoma cell lines were used in the study. The half-maximal inhibitory concentration (IC50) values of cisplatin and the investigated compounds evaluated after 72 h of drug exposure are depicted in Table 2 and Fig. 4. Series 1 [square planar Pt(II) compounds] and series 2 an 3 [octahedral Pt(IV) compounds] exhibited remarkable cytotoxicity in all the carcinoma cell lines selected, although showing great differences in their cytotoxic effectiveness. Cyclometallated Pt(IV) series 2, with CH3/I as axial ligands, showed the lowest IC50 values of the series and special sensitivity for A-549 lung (1.42–2.62 μM) and HCT-116 colon (1.26–5.43 μM) and MDA-MB-231 (2.06–3.45 μM) breast cancer cells. Compound 2c, exhibiting an iodido group in trans to the imine nitrogen, was approximately up to 3.5-, 5- and 5-fold more potent than cisplatin itself in A-549 lung, HCT-116 colon and MDA-MB-231 breast cells, respectively. Interestingly, considering the breast adenocarcinoma cells (MDA-MB-231 and MCF-7), series 2 showed stronger selectivity for the triple negative (ER, PR and HER2 negative) MDA-MB-231 (2.34–3.45 μM) than for the ER and PR positive MCF7 (6.90–37.78 μM) cancer cells.

DNA interaction in the presence or absence of ascorbic acid

The interaction of cyclometallated Pt(II) (1a–1c) and cyclometallated Pt(IV) (2a–2c and 3a–3c) complexes with DNA was assessed by their ability to modify the electrophoretic mobility of the supercoiled closed circular (sc) and the open circular (oc) forms of pBluescript SK+ plasmid DNA. The sc form usually moves faster due to its compact structure.

Fig. 5 shows the electrophoretic mobility of pBluescript SK+ plasmid DNA incubated with cyclometallated series 1, 2 and 3 at increasing concentrations. For comparison, the incubation of DNA with cisplatin and ethidium bromide (EB) was also performed.

As was expected, based on the previous results, square planar platinacycles 1a–1c alter the mobility of plasmid DNA (Fig. 5), especially compound 1c. A decrease in mobility was observed at quite high concentrations tested in the experiment (up to 50 μM for compound 1c and 100 μM for compounds 1a and 1b). For comparison, the reference cisplatin modifies the DNA electrophoretic migration at a considerably much lower concentration (2.5 μM). On the basis of this gel mobility shift assay, it is hypothesized that platinacycles 1a–1c alter the DNA tertiary structure by the same mechanism as the standard reference, cisplatin, but at higher concentrations. In contrast with these findings, octahedral Pt(IV) compounds 2a–2c and 3a–3c (Fig. 5) did not modify the plasmid DNA electrophoretic mobility, pointing to a different mechanism of action or an alternative biomolecular target. It is worth mentioning

253 that Pt(II) compounds, triggering the greatest effect in the DNA tertiary structure, were not the more
254 cytotoxic agents of the studied series.
255 In order to investigate the effect of ascorbic acid on the in vitro activity of the octahedral platinum(IV)
256 compounds 2a–2c and 3a–3c, further experiments were conducted. Supercoiled pBluescript SK+
257 plasmid DNA was co-incubated with series 2 and 3 (0–200 μM) in the absence and presence of ascorbic
258 acid (500 μM) at 37 °C for 24 h (Fig. 6). No alteration on the DNA electrophoretic mobility was
259 observed for the Pt(IV) compounds investigated at any of the concentrations tested. Hence it is assumed
260 that no reduction took place to yield the corresponding platinum(II) cyclometallated compounds 1a–1c,
261 which were able to modify the DNA migration in the previous electrophoretograms.
262 These results were in accordance with the above 1H NMR experiments performed in the presence of
263 ascorbic acid (aqueous solution at pH = 7.40). The reluctance of the Pt(IV) cyclometallated compounds
264 under study (2a–2c and 3a–3c) to be reduced is also in agreement with the previously published results
265 on Pt(IV) cyclometallated compounds.17
266
267 **Topoisomerase inhibition**
268 Topoisomerases are essential nuclear enzymes that maintain the topological change of DNA and play a
269 key role in transcription, replication and chromosome segregation.44 Human DNA topoisomerases (topo
270 I and topo II) are expressed at different levels in different cancer types. For instance, topo I is
271 overexpressed in colon cancer cell lines, while topo II is overexpressed in breast and ovarian cancer cell
272 lines.45 Camptothecin and etoposide, topo I and topo II inhibitor, respectively, are clinically approved
273 anticancer drugs. Human topoisomerases operate in two different ways. One causes single-strand breaks
274 (SSBs, called type I), and the other induces double-strand breaks (DSBs, type II), during cell
275 proliferation processes. Between these two types of topoisomerases, topoisomerase II is essential to
276 relax supercoiled DNA through a catalytic cycle of DSBs.45 There are two isoforms of topoisomerase
277 II, α and β forms. Despite their similarities, the two enzymes have distinct patterns of expression and
278 physiological functions in vertebrate cells. The expression level of topoisomerase IIα is up-regulated
279 dramatically during cell proliferation. 46 It is found at replication forks and remains tightly associated
280 with chromosomes during mitosis.47 In contrast, the expression of the β isoform is independent of the
281 proliferative status of cells and the enzyme dissociates from chromosomes during mitosis.48 Therefore,
282 topoisomerase IIα has been considered as a more attractive target than topoisomerase IIβ for the
283 development of chemotherapeutic agents.47
284 To evaluate the ability of the platinum(IV) complexes 2a–2c and 3a–3c to inhibit topoisomerase I or to
285 intercalate into DNA, a topoisomerase-based gel assay was performed.49 Supercoiled pBluescript
286 plasmid DNA was incubated in the presence of topoisomerase I at increasing concentrations of
287 compounds 2 and 3. Ethidium bromide (EB), used as an intercalator control, prevents the shift of
288 supercoiled DNA into a relaxed state. The results showed that none of the investigated compounds

289 prevent unwinding of DNA by the action of topoisomerase I, indicating that the compounds are neither
290 intercalators nor the topoisomerase I inhibitor (not shown).
291 To evaluate the ability of the platinum(IV) complexes 2a–2c and 3a–3c to inhibit topoisomerase Iiα, a
292 similar topoisomerase-based gel assay was performed.50 Supercoiled pBluescript plasmid DNA was
293 incubated in the presence of topoisomerase IIα at increasing concentrations of compounds series 2 and
294 3. Etoposide was used as a control of the topo IIα inhibitor. Fig. 7 summarizes the topo IIα inhibitory
295 activity of the assayed compounds. Platinum(IV) complex 3c showed strong topo IIα inhibitory activity
296 at 100 μM and platinum(IV) complexes 2b and 3a showed considerable topo IIα inhibitory activity at 20
297 μM. These results are very remarkable, taking into account that, under the conditions of the experiment,
298 platinacycles 2b, 3a and 3c, in particular 2b and 3a, are by far more potent than the anticancer marketed
299 drug etoposide. Further experiments are ongoing to study the poison or catalytic character of the
300 synthesized topo IIα inhibitors.
301 Cathepsin B inhibition Cathepsin B is a metalloprotease that has been proposed to participate in
302 metastasis, angiogenesis, and tumor progression in solid tumors. Recently, an excellent correlation
303 between cathepsin B inhibition and cytotoxicity for some metallacycles has been reported.51 It should
304 be noted that platinum(IV) compound 3a inhibits cathepsin B (IC50 = 55 ± 4 μM). In contrast, while
305 compounds 3b and 3c present a very similar chemical structure, platinum(II) compounds 1a–1c and
306 platinum(IV) compounds 2a–2c did not show any significant cathepsin B inhibitory activity.
307
308 **Effect of compounds 2b and 2c on cell cycle distribution**
309 Cell cycle is the organized and monitored process between two mitotic divisions which assure the proper
310 cell proliferation.52 Cell cycle distribution basically consists of three main phases: quiescent and gap1
311 (G0 and G1), synthesis (S), and gap2 and mitosis (G2 and M) phases. It is a very tightly regulated set of
312 events that involves various checkpoints and several proteins which are proposed as antitumor targets,
313 and any disruption in this machinery causes oncogenesis.52–54 The effect of compounds 2b and 2c (as
314 representative examples of platinum(IV) compounds) on the cell cycle distribution was studied over the
315 A-549 lung cancer cell line. A-549 cells were incubated with these compounds at their half maximal
316 inhibitory concentrations (IC50) for 72 h and then analyzed by Fluorescence Activated Cell Sorting
317 (FACS) using propidium iodide (PI) staining to quantify the DNA content of each cell population. As
318 shown in Fig. 8, it is observed that both compounds have a similar decrease in the G0/G1 and G2 phases
319 while they lead to a significant arrest in the S phase of the cell cycle distribution (over 20%) where the
320 cells supposedly stop DNA replication.
321
322 **Effect of compounds 2b and 2c on apoptosis induction**
323 Organisms have evolved in a way that unhealthy or damaged cells are eliminated from the body in a
324 programmed cell death mechanism known as apoptosis. Unlike healthy cells, as a cancer hallmark,
325 cancer cells often avoid the apoptotic stimuli which are caused under increased stress conditions.55,56

326 Therefore, chemotherapeutic-induced apoptosis is of great interest in cancer therapy. On the other hand,
327 any alteration in the cell cycle may induce apoptosis,57 and therefore, the apoptotic properties of
328 compounds 2b and 2c (as representative examples of platinum(IV) compounds) in the A-549 cell line
329 were investigated. A-549 cells were incubated with these compounds at their half maximal inhibitory
330 concentrations (IC50) for 72 h and then analyzed by flow cytometry using fluorescein- labeled annexin
331 V (AV-FITC, annexin V-fluorescein isothiocyanate) and propidium iodide (PI) staining.
332 Apoptosis starts with the loss of plasma membrane symmetry, and phosphatidylserine (PS) is
333 translocated from the inner membrane to the outer. In this way, the externally exposed PS can bind to
334 the annexin V-FITC conjugate with a high affinity in the outer environment of the cell. The integrity of
335 the cell membrane is lost at the late apoptotic/necrotic stages, thus allowing PI to access the nucleus and
336 intercalate between the DNA bases.58,59 Flow cytometry analysis with annexin V-FITC staining and PI
337 accumulation was used to distinguish the non-apoptotic cells (annexin V− and PI−), early apoptotic cells
338 (annexin V+ and PI−) and late apoptotic/necrotic cells (PI+).
339 As shown in Fig. 9, both compounds have high apoptotic effects on A-549 cells. Treatment with
340 compound 2b at its half maximal inhibitory concentrations (IC50) for 72 h resulted in 80% decrease in
341 the healthy cell population while early apoptotic and necrotic populations increased significantly (35%
342 and 44%, respectively). Similarly, treatment with compound 2c at its half maximal inhibitory
343 concentrations (IC50) for 72 h resulted in around 20% decrease in healthy cell population and the
344 population of early apoptotic cells has increased around 20%. Compound 2c did not induce any
345 significant necrosis. These results indicate that both compounds, 2b and 2c, have highly potent
346 antiproliferative effects on the A-549 lung cancer cells. The mechanism of action of the compounds is a
347 combination of cell cycle arrest and particularly apoptosis induction. Compound 2c mostly induces an
348 increase in the population of early apoptotic cells, while 2b induces an increase both in apoptotic and
349 necrotic cells, hence indicating the potential of these compounds to be used in cancer chemotherapy.
350

351 **Generation of reactive oxygen species (ROS)**

352 Reactive oxygen species (ROS) include molecules with increased reactivity such as superoxide (O2 −),
353 hydrogen peroxide (H2O2), hydroxyl radical (•OH) and singlet oxygen (1O2) and are produced in all
354 cells as normal metabolic by-products. The effect of ROS on cells depends on its concentration, and low
355 ROS concentrations are reported not only to contribute to cell survival and proliferation as it plays a role
356 in post translational modification of phosphatases and kinases60,61 but also to be required for
357 homeostatic signaling events, cell differentiation and cell mediated immunity. While moderate ROS
358 levels lead to the expression of some stress responsive genes involving HIF-1, which in turn triggers the
359 expression of prosurvival proteins,62 high ROS levels may induce severe damage to several cellular
360 macromolecules involving proteins, lipids, nuclear and mitochondrial DNA and cause the induction of
361 cell senescence or crisis.63 High ROS levels may also lead to permeabilization of mitochondria which
362 causes the release of cytochrome c and in turn, apoptosis.64 It has been reported that ROS may play an

important role in cisplatin-induced cytotoxicity65 since cisplatin is known to produce ROS.66 Nevertheless, the ROS formation of platinum(IV) complexes has not been studied widely so far. In this study, the amount of ROS generated by compounds 2b and 2c (as representative examples of platinum(IV) compounds) in the A-549 cell line was investigated. A-549 cells were incubated with these compounds at their half maximal inhibitory concentrations (IC50) for 72 h and then analyzed by flow cytometry using the DFCH-DA (2′,7′-dichlorofluorescein diacetate) assay. As shown in Fig. 10, compound 2b did not cause significant ROS generation while the production of ROS in A-549 cells incubated with compound 2c increased significantly compared to control cells. These results are in accordance with the previous studies exhibiting that certain platinum(IV) complexes are able to induce elevated ROS levels as part of their biological activities in cancer cells.17,67,68

CONCLUSIONS

A systematic method to prepare novel octahedral cyclometallated platinum(IV) compounds containing one, two or three labile iodido ligands is presented. Six new cyclometallated platinum(IV) compounds including two geometrical isomers (2c and 3b) were prepared from the intermolecular oxidative addition of methyl iodide (compounds 2a–2c) or iodine (compounds 3a–3c) to cyclometallated platinum(II) compounds [PtX {(CH3)2N(CH2)3NCH(4-ClC6H3)}] (1a–1c: X = Cl, CH3 or I). All compounds were characterized by NMR spectroscopy and elemental analyses. The molecular structures of platinum(II) compound 1c and platinum(IV) compounds 3b and 3a′ (an isomer of 3a) were solved by X ray analyses. The cytotoxic activity against a panel of human adenocarcinoma cell lines (A-549 lung, MDA-MB-231 and MC-7 breast, and HCT-116 colon) was determined for these compounds and the cyclometallated platinum(II) precursors. All compounds exhibited a remarkable cytotoxicity in all the selected cancer cell lines and cyclometallated compounds 2a–2c containing a methyl and an iodido axial ligand are the most potent. The electrophoretic mobility of platinum(II) compounds 1a–1c indicates alteration of the DNA tertiary structure in a similar way to cisplatin, although at higher concentrations. In contrast, platinum(IV) compounds 2a–2c and 3a–3c were not effective at all for removing the plasmid DNA supercoils, not even in the presence of ascorbic acid. Consistently, 1H NMR experiments carried out for 2b and 2c did not show evidence of reduction in the presence of ascorbic acid. Topoisomerase-based gel assays indicated that none of the compounds 2a–2c and 3a–3c were topoisomerase I inhibitors, but compounds 2b and 3a, and to a lesser extent 3c showed considerable topo IIα inhibitory activity. In addition, compound 3a inhibits cathepsin B. Compounds 2b and 2c were found to supress A-549 lung cancer cell growth by a combination of cell cycle arrest and apoptosis induction. Moreover, compound 2c can induce the ROS levels. As a whole, these studies indicate that these new cyclometallated platinum(IV) compounds containing iodide ligands display a high potential to be used in cancer chemotherapy. Their biological properties can be tuned by a careful choice of the nature, number and arrangement of the iodide ligands in the coordination sphere of platinum(IV).

402 **EXPERIMENTAL SECTION**

403

404 **Chemistry**

405 General. Microanalyses were performed at the Centres Científics i Tecnològics (Universitat de
406 Barcelona). Mass spectra were performed at the Unitat d'Espectrometria de Masses (Universitat de
407 Barcelona) in a LC/MSD-TOF spectrometer using H2O–CH3CN 1 : 1 to introduce the sample. NMR
408 spectra were performed at the Unitat de RMN d'Alt Camp de la Universitat de Barcelona using a
409 Mercury-400 (1H, 400 MHz; 13C, 100.6 MHz) or a Bruker 400 Avance III (195Pt, 85.68 MHz) and
410 referenced to SiMe4 (1H and 13C) or to H2PtCl6 in D2O (195Pt). δ values are given in ppm and J
411 values in Hz. Abbreviations used: s = singlet; d = doublet; t = triplet; m = multiplet.

412 **Preparation of the complexes.** All reagents were obtained from commercial sources and used as
413 received. Ligand 4-ClC6H4CHN(CH2)3N(CH3)2 36 and compounds [Pt2(CH3)4{μ-S(CH3)2}2],69
414 cis-[PtI2(dmso)2],41 and [PtCl{(CH3)2N(CH2)3NCH (4-ClC6H3)}]36 (1a) were prepared as reported
415 elsewhere. Compound 1a was purified by column chromatography using SiO2 as the stationary phase
416 and dichloromethane–methanol (100 : 1) as the eluent.

417 [**Pt(CH3){(CH3)2N(CH2)3NCH(4-ClC6H3)}] (1b)** was obtained from 0.207 g (0.4 mmol) of
418 [Pt2(CH3)4{μ-S(CH3)2}2] and 0.146 g (0.7 mmol) of imine 4-ClC6H4CHN(CH2)3N(CH3)2, dissolved
419 in toluene (40 mL). The mixture was refluxed for 1 hour obtaining a red-garnet solution. The solvent
420 was removed and the solid was treated with diethyl ether (5 mL) and filtered. Yield: 0.227 g (64%). 1H-
421 NMR (400 MHz, CDCl3): δ 8.56 [s, 3J (Pt–H) = 59.6, 1H, Hd] δ 7.63 [d, 3J (Pt–H) = 65.2, 4J(H–H) =
422 1.6, 1H, Ha] δ 7.18 [d, 3J(H–H) = 8.0, 1H, Hc] δ 6.95 [dd, 3J(H–H) = 8.0, 4J(H–H) = 2.0, 1H, Hb] δ
423 3.85 [t, 3J(H–H) = 4.6, 2H, He] δ 2.91 [m, 2H, Hg] δ 2.73 [s, 3J (Pt–H) = 23.6, 6H, Hh] δ 2.02 [qi,
424 3J(H–H) = 5.1, 2H, Hf] δ 0.99 [s, 2J (Pt–H) = 80.8, 3H, Hi]. 13C-NMR (100.6 MHz, CDCl3): δ 171.6
425 [2J (Pt–C) = 82.1, Cd] δ 146.4, 144.9, 136.8 [Caromatics] δ 132.8 [Ca] δ 128.5 [3J (Pt–C) = 45.9, Cc] δ
426 122.1 [Cb] δ 65.1 [Cf] δ 56.4 [Ce] δ 49.8 [Ch] δ 27.58 [Cg] δ 10.53 [Ci]. 195Pt-NMR (85.68 MHz,
427 CDCl3): −3735.55 [s]. Anal. calc. for C13H19ClN2Pt (%): C, 35.99; H, 4.41; N, 6.46. Found (%): C,
428 35.71; H, 4.58; N, 6.19.

429 **[PtI{(CH3)2N(CH2)3NCH(4-ClC6H3)}] (1c)** was obtained from 0.426 g (0.70 mmol) of cis-
430 [PtI2(dmso)2], 0.158 g (0.75 mmol) of imine 4-ClC6H4CHN(CH2)3N(CH3)2 and 0.063 g (0.77 mmol)
431 of sodium acetate dissolved in methanol (30 mL). The mixture was refluxed for 48 hours, then the
432 solvent was removed and the solid was extracted with dichloromethane (20 mL) to yield a dark red
433 solution that was evaporated to dryness. The residue was recrystallized at room temperature from
434 dichloromethane– methanol. Yield: 0.166 g (44%). Alternatively, compound 1c – slightly impure with
435 traces of 1a according to the 1H NMR spectrum – was obtained from 1a. 76 mg (0.17 mmol) of 1a were
436 dissolved in 15 mL of dichloromethane and a solution of AgNO3 (34 mg, 0.20 mmol) in 5 mL of
437 methanol was added. After stirring for one hour, the mixture was filtered and 60 mg (0.36 mmol) of KI
438 were added. After stirring for 30 minutes, the solvent was removed and the residue was recrystallized in

dichloromethane–methanol. Yield 0.160 g (42%). 1H-NMR (400 MHz, CDCl3): δ 8.75 [d, 3J (Pt–H) = 48.6, 4J(H–H) = 2.0, 1H, Ha] δ 8.42 [s, 3J (Pt–H) = 139.0, 1H, Hd] δ 7.18 [d, 3J(H–H) = 8.0, 1H, Hc] δ 6.95 [dd, 3J(H–H) = 8.1, 4J(H–H) = 2.0, 1H, Hb] δ 3.84 [td, 3J (Pt–H) = 33.9, 3J(H–H) = 4.6, 4J(H–H) = 1.6, 2H, He] δ 3.01 [s, 3J (Pt–H) = 16.7, 6H, Hh] δ 2.82 [m, 2H, Hg] δ 2.06 [m, 2H, Hf]. HRMS-ESI-(+) {H2O :CH3CN (1 : 1)}, m/z: 459.0897 (calc. for C14H19N3ClPt 459.0909) [M − NH4 + CH3CN]+. Anal. calc. for C12H16ClIN2Pt (%): C, 26.41; H, 2.96; N, 5.13. Found (%): C, 27.60; H, 3.09; N, 5.25.

[Pt(CH3)ClI{(CH3)2N(CH2)3NCH(4-ClC6H3)}] (2a) was obtained from 0.050 g (0.11 mmol) of the cyclometallated [PtCl{(CH3)2N(CH2)3NCH(4-ClC6H3)}] 1a dissolved in acetone. 1 mL of CH3I was added and the mixture was stirred for 24 hours. After this time, the solvent was removed, the residue was washed with diethyl ether (10 mL) and the yellow solid was filtered under vacuum. Yield: 0.034 g (52%). 1H-NMR (400 MHz, acetone-d6): δ 8.77 [t, 3J (Pt–H) = 116.4, 4J(H–H) = 1.8, 1H, Hd] δ 7.94 [d, 3J (Pt–H) = 32.4, 4J(H–H) = 2.0, 1H, Ha] δ 7.66 [d, 4J (Pt–H) = 4.8, 3J(H–H) = 8.4, 1H, Hc] δ 7.22 [dd, 3J(H–H) = 8.0, 4J(H–H) = 2.0, 1H, Hb] δ 4.30 [m, 2H, He] δ 3.43 [s, 3J (Pt–H) = 11.6, 3H, Hh] δ 2.93 [m, 2H, Hg] δ 2.67 [s, 3J (Pt–H) = 15.2, 3H, Hh′] δ 2.21 [m, 2H, Hf] δ 1.54 [s, 3J (Pt–H) = 64.8, 3H, Hj]. Anal. calc. for C13H19Cl2IN2Pt·H2O (%): C, 25.42; H, 3.44; N, 4.56. Found (%): C, 24.93; H, 3.02; N, 4.27.

[Pt(CH3)2I{(CH3)2N(CH2)3NCH(4-ClC6H3)}] (2b) was prepared from 0.080 g (0.2 mmol) of [PtCH3{(CH3)2N(CH2)3NCH (4-ClC6H3)}] 1b using the same procedure and a reaction time of 1 hour. Yield: 0.071 g (67%). 1H-NMR (400 MHz, CDCl3): δ 8.39 [s, 3J (Pt–H) = 47.6, 1H, Hd] δ 7.39 [d, 3J (Pt–H) = 47.0, 3J(H–H) = 8.0, 1H, Ha] δ 7.32 [d, 4J (Pt–H) = 7.6, 3J(H–H) = 8.0, 1H, Hc] δ 7.03 [dd, 3J(H–H) = 8.0, 4J(H–H) = 1.9, 1H, Hb] δ 4.25 [tt, 3J(H–H) = 13.2, 4J(H–H) = 2.6, 1H, He] δ 3.98 [dt, 2J(H–H) = 15.2, 3J(H–H) = 4.2, 1H, He′] δ 3.60 [m, 1H, Hg] δ 3.19 [s, 3J (Pt–H) = 13.2, 3H, Hh] δ 2.71 [m, 1H, Hg′] δ 2.43 [s, 3J (Pt–H) = 17.2, 3H, Hh′] δ 2.05 [m, 2H, Hf] δ 1.38 [s, 2J (Pt–H) = 66.0, 3H, Hi] δ 0.79 [s, 2J (Pt–H) = 69.2, 3H, Hj]. In addition, resonances corresponding to a minor isomer (<10%) were observed at δ 8.45 [s, 3J (Pt–H) = 40.0, 1H, Hd] δ 7.38 [d, 3J(H–H) = 8.0, 1H, Ha] δ 7.07 [dd, 3J(H–H) = 8.0, 4J(H–H) = 2.0, 1H, Hb] δ 2.93 [s, 3J (Pt–H) = 16.0, 3H, Hh] δ 2.45 [s, 3J (Pt–H) = 16.0, 3H, Hh′] δ 1.23 [s, 2J (Pt–H) = 65.3, 3H, Hi] δ 0.61 [s, 2J (Pt–H) = 71.5, 3H, Hj]. Anal. calc. for C14H22ClN2Pt (%): C, 29.20; H, 3.85; N, 4.87. Found (%): C, 29.00; H, 4.01; N, 4.65.

[Pt(CH3)I2{(CH3)2N(CH2)3NCH(4-ClC6H3)}] (2c) was prepared from 0.060 g (0.11 mmol) of [PtI{(CH3)2N(CH2)3NCH(4- ClC6H3)}] 1c using the same procedure and a reaction time of 24 hours. Yield: 0.066 g (73%). 1H-NMR (400 MHz, CDCl3): δ 8.75 [d, 3J (Pt–H) = 39.8, 4J(H–H) = 1.8, 1H, Ha] δ 8.22 [s, 3J (Pt–H) = 104.0, 1H, Hd] δ 7.36 [d, 4J (Pt–H) = 4.8, 3J(H–H) = 8.4, 1H, Hc] δ 7.08 [dd, 3J(H–H) = 8.1, 4J(H–H) = 1.9, 1H, Hb] δ 4.39 [m, 1H, He] δ 3.72 [d, J(H–H) = 17.0,1H, He′] δ 3.64 [s, 3J (Pt–H) = 13.9, 3H, Hh] δ 3.42 [m, 1H, Hf] δ 2.72 [s, 3J (Pt–H) = 16.1, 3H, Hh′] δ 2.65 [m, 1H, Hf′] δ 2.18 [m, 1H, Hg′] δ 2.07 [m, 1H, Hg] δ 1.71 [s, 3J (Pt–H) = 65.5, 3H, Hj]. ESI-MS(+): 560.9914 [M − I]+. Anal. calc. for C13H19ClI2N2Pt (%): C, 22.71; H, 2.79; N, 4.07. Found (%): C, 23.11; H, 2.83; N, 4.28.

[PtClI2{(CH3)2N(CH2)3NCH(4-ClC6H3)}] (3a) was obtained from 0.039 g (0.1 mmol) of the cyclometallated [PtCl{(CH3)2 N(CH2)3NCH(4-ClC6H3)}] 1a dissolved in acetone (15 mL) and 0.023 g (0.1 mmol) of I2 dissolved in acetone (6 mL). The solution was stirred for 75 minutes, the solvent was removed and 10 mL of diethyl ether were added. The obtained solid was filtered under vacuum. Yield: 0.055 g (90%). 1H-NMR (400 MHz, CDCl3): δ 7.92 [s, 3J (Pt–H) = 95.2, 1H, Hd] δ 7.91 [s, 3J (Pt–H) = 28.0, 1H, Ha] δ 7.46 [d, 3J(H–H) = 8.1, 1H, Hc] δ 7.00 [dd, 3J(H–H) = 8.1, 4J(H–H) = 1.9, 1H, Hb] δ 4.11 [td, 3J(H–H) = 5.3, 4J(H–H) = 1.3, 2H, He] δ 3.44 [s, 3J (Pt–H) = 14.8, 6H, Hh] δ 3.02 [m, 2H, Hg] δ 2.26 [m, 2H, Hf]. In addition, resonances corresponding to a minor isomer (<10%) were observed at δ 8.09 [s, 1H, Hd] δ 7.97 [d, 4J(H–H) = 2.0, 1H, Ha] δ 7.45 [d, 3J(H–H) = 8.1, 1H, Hc] δ 7.13 [dd, 3J(H–H) = 8.0, 4J(H–H) = 2.0, 1H, Hb] δ 3.27 [s, 3J (Pt–H) = 16.0, 6H, Hh]. Anal. calc. for C12H16Cl2I2N2Pt (%): C, 20.36; H, 2.28; N, 3.96. Found (%): C, 20.27; H, 2.32; N, 4.00.

[Pt(CH3)I2{(CH3)2N(CH2)3NCH(4-ClC6H3)}] (3b) was prepared following the same procedure from 0.080 g (0.2 mmol) of [PtCH3{(CH3)2N(CH2)3NCH(4-ClC6H3)}] 1b and 0.047 g (0.2 mmol) of I2. Yield: 0.087 g (69%). 1H-NMR (400 MHz, CDCl3): δ 8.16 [s, 3J (Pt–H) = 46.8, 1H, Hd] δ 7.30 [d, 3J(H–H) = 8.0, 1H, Hc] δ 7.21 [d, 3J (Pt–H) = 36.0, 4J(H–H) = 1.8, 1H, Ha] δ 6.85 [dd, 3J(H–H) = 8.0, 4J(H–H) = 1.9, 1H, Hb] δ 4.04 [td, 3J (Pt–H) = 20.8, 3J(H–H) = 5.5, 4J(H–H) = 1.7, 2H, He] δ 3.11 [s, 3J (Pt–H) = 17.6, 6H, Hh] δ 3.05 [m, 2H, Hg] δ 2.21 [s, 3J (Pt–H) = 69.2, 3H, Hi] δ 2.15 [m, 2H, Hf]. Anal. calc. for C13H19ClI2N2Pt (%): C, 22.71; H, 2.79; N, 4.07. Found (%): C, 22.94; H, 2.90; N, 3.99.

[PtI3{(CH3)2N(CH2)3NCH(4-ClC6H3)}] (3c) was prepared following the same procedure from 0.080 g (0.11 mmol) of [PtI{(CH3)2N(CH2)3NCH(4-ClC6H3)}] 1c and 0.028 g (0.11 mmol) of I2 and a reaction time of 2 hours. Yield: 0.073 g (83%). 1H-NMR (400 MHz, CDCl3): δ 8.49 [d, 3J (Pt–H) = 32.7, 4J(H–H) = 1.9, 1H, Ha] δ 7.99 [t, 3J (Pt–H) = 88.0, 4J(H–H) = 1.6, 1H, Hd] δ 7.42 [d, 3J(H–H) = 8.1, 1H, Hc] δ 6.93 [dd, 3J(H–H) = 8.1, 4J(H–H) = 1.9, 1H, Hb] δ 3.97 [td, 3J(H–H) = 5.3, 4J(H–H) = 1.6, 2H, He] δ 3.57 [s, 3J (Pt–H) = 16.8, 6H, Hh] δ 2.93 [m, 2H, Hg] δ 2.33 [m, 2H, Hf]. ESI-MS(+): 800.7796 [M + H]+. Anal. calc. for C12H16ClI3N2Pt (%): C, 18.03; H, 2.01; N, 3.51. Found (%): C, 18.41; H, 2.01; N, 3.51.

Stability and behavior in the presence of ascorbic acid by NMR measurements

The stability of the platinum(IV) compounds under investigation in aqueous solution was monitored by 1H NMR spectroscopy at ambient temperature. Samples were analyzed in the Nuclear Magnetic Resonance Unit, Scientific and Technological Centers of the University of Barcelona (CCiTUB). The solutions of the complexes were prepared in 50 mM phosphate buffer (in D2O, pD 7,40) and a minimum amount (2 drops) of d6-DMSO for the solubilization of the compound. The final concentration of the complex was 1 mM and 1H NMR spectra were recorded with a Varian 400 and a Bruker 400 spectrometer at time periods between 0 h and 10 days. For monitoring the reactivity of the studied compounds with ascorbic acid, the samples were prepared under the same conditions as described above

512 with a final concentration of the complex and ascorbic acid of 1 mM and 25 mM, respectively. 1H NMR
513 spectra were recorded over the same time period as described above.
514 The stability of compound 2b in aqueous solution: the resonances assigned to the single species initially
515 formed and stable up to ten days are given. δ = 8.59 [s, 3J(H–Pt) = 52, imine], {7.38 [d], 7.27 [s], 7.10
516 [d], aromatics}, {0.92 [s, 3J(H–Pt) = 64], 0.65 [s, 3J(H–Pt) = 80], MePt}. The reactivity of compound
517 2b with ascorbic acid in aqueous solution: the resonances assigned to a single species initially formed
518 and stable up to ten days are given. δ = 8.59 [s, 3J(H–Pt) = 52, imine], {7.38 [d], 7.27 [s], 7.10 [d],
519 aromatics}, {0.92 [s, 3J(H–Pt) = 64], 0.45 [s, 3J(H–Pt) = 56], MePt}.
520 The stability of compound 2c in aqueous solution: the resonances assigned to two observed species are
521 given. Initial compound: δ = 8.26 [s, imine], {8.49 [d, Ha], 7.45 [d], 7.18 [d], aromatics}, 1.52 [s, MePt].
522 The second compound is formed and its relative intensity increases with time. δ = 8.34 [s, imine], {7.25
523 [d], 6.98 [dd], aromatics}, 1.10 [s, MePt].
524 The reactivity of compound 2c with ascorbic acid in aqueous solution: the resonances assigned to a
525 single species initially formed and stable up to 72 hours are given. δ = 7.75 [s, imine], {8.26 [d, Ha],
526 7.25 [d], 7.08 [d], aromatics}, 1.10 [s, MePt].
527
528 **X-ray diffraction**
529 Suitable crystals of compounds 1c, 3b and 3a′ were grown at room temperature in dichloromethane–
530 methanol. X-ray diffraction data were collected for prism-like specimens on a D8 VENTURE system
531 equipped with a multilayer monochromator and a Mo high brilliance Incoatec Microfocus Source (λ =
532 0.71073 Å) at 100 K (1c and 3b) or at 293 K (3a′). The structures were solved and refined using the
533 Bruker SHELXTL software package.70 Crystallographic details are given in Table 3.
534
535 **Biological studies**
536 **Cell culture and cell viability assay.** Human lung adenocarcinoma A-549 cells and human breast
537 adenocarcinoma cells were grown as a monolayer culture in minimum essential medium (DMEM with
538 L-glutamine, without glucose and without sodium pyruvate) with the addition of 10% heat-inactivated
539 Fetal Calf Serum (FCS), 10 mM D-glucose and 0.1% streptomycin/penicillin, under standard culture
540 conditions (humidified air with 5% CO2 at 37 °C). Human breast adenocarcinoma MCF-7 cells were
541 cultured in MEM without phenol red, containing 10% Fetal Bovine Serum (FBS), 10 mM D-glucose, 1
542 mM sodium pyruvate, 2 mM L-glutamine, 0.1% streptomycin/penicillin, 0.01 mg mL−1 insulin, and 1%
543 nonessential amino acids. Human colorectal carcinoma HCT116 cells were cultured in a DMEM/HAM
544 F12 (1 : 1 volume) mixture containing 10% FBS, 4 mM L-glutamine, 12.5 mM D-glucose and 0.1%
545 streptomycin/penicillin.
546 For all viability assays, compounds were suspended in high purity DMSO at 20 mM as a stock solution.
547 To obtain the final assay concentrations, they were diluted in DMEM (Dulbecco's Modified Eagle's
548 Medium) (the final concentration of DMSO was the same for all conditions, and was always lower than

549 1%). The assay was performed by a variation of the MTT (3-(4,5-dimethylthiazol-2-yl)-2,5-
550 diphenyltetrazolium bromide) assay described by Mosmann et al.71 and Matito and coworkers72 which
551 is based on the ability of live cells to cleave the tetrazolium ring of the MTT thus producing formazan,
552 which absorbs at 550 nm. In brief, the corresponding number of cells per well (2.5 × 103 A-549 cells per
553 well, 5 × 103 MDA-MB-231 cells per well, 1 × 104 MCF-7 cells per well and 2 × 103 HCT-116 cells
554 per well) were cultured in 96 well plates for 24 hours prior to the addition of different compounds at
555 different concentrations, in triplicate. After incubation of the cells with the compounds for 72 h more,
556 the media were aspirated and 100 μL of filtered MTT (0.5 mg mL−1) were added to each well.
557 Following 1 h of incubation with the MTT, the supernatant was removed and the precipitated formazan
558 was dissolved in 100 μL DMSO. Relative cell viability, compared to the viability of untreated cells, was
559 measured by absorbance at 550 nm on an ELISA plate reader (Tecan Sunrise MR20-301, TECAN,
560 Salzburg, Austria). Concentrations that inhibited cell growth by 50% (IC50) after 72 h of treatment were
561 subsequently calculated.
562
563 **DNA migration studies**
564 A stock solution (10 mM) of each compound was prepared in high purity DMSO. Then, serial dilutions
565 were made in MilliQ water (1 : 1). Plasmid pBluescript SK+ (Stratagene) was obtained using a
566 QIAGEN plasmid midi kit as described by the manufacturer. The interaction of drugs with pBluescript
567 SK+ plasmid DNA was analysed by agarose gel electrophoresis following a modification of the method
568 described by Abdullah et al.73 Plasmid DNA aliquots (40 μg mL−1) were incubated in TE buffer (10
569 mM Tris-HCl, 1 mM EDTA, pH 7.5) with different concentrations of compounds 1a–1c, 2a–2c and 3a–
570 3c, ranging from 0 μM to 200 μM at 37 °C for 24 h. The final DMSO concentration in the reactions was
571 always lower than 1%. For comparison, cisplatin and ethidium bromide (EB) were used as reference
572 controls. The aliquots of 20 μL of the incubated solutions containing 0.8 μg of DNA were subjected to
573 1% agarose gel electrophoresis in TAE buffer (40 mM tris-acetate, 2 mM EDTA, pH 8.0). The gel was
574 stained in TAE buffer containing ethidium bromide (0.5 mg mL−1) and visualized and photographed
575 under UV light.
576 The same experimental procedure was carried out incubating plasmid DNA with the platinum(IV)
577 complexes 2a–2c and 3a–3c (25–200 μM) in the absence or presence of ascorbic acid (500 μM) in a
578 0.1× Tris-EDTA buffer (pH 7.8) for 24 h at 37 °C, as described elsewhere.67
579
580 **Topoisomerase inhibition assays**
581 Topoisomerase I-based experiments were performed as described previously.49 Supercoiled pBluescript
582 DNA, obtained as described above, was treated with topoisomerase I in the absence or presence of
583 increasing concentrations of compounds 2a–2c and 3a–3c. Assay mixtures contained supercoiled
584 pBluescript DNA (0.8 μg), calf thymus topoisomerase I (3 units) and complexes 2a–2c and 3a–3c (0–
585 100 μM) in 20 μL of relaxation buffer Tris-HCl buffer (pH 7.5) containing 175 mM KCl, 5 mM MgCl2

586 and 0.1 mM EDTA. Ethidium bromide (EB, 10 μM) was used as a control of intercalating agents and
587 etoposide (E, 100 μM) as a control of the non-intercalating agent. Reactions were incubated for 30 min
588 at 37 °C and stopped by the addition of 2 μL of agarose gel loading buffer. Samples were then subjected
589 to electrophoresis and DNA bands were stained with ethidium bromide as described above.
590 The DNA topoisomerase IIα inhibitory activity of the compounds tested in this study was measured as
591 described elsewhere50 with a few modifications. Supercoiled pBluescript DNA was incubated with
592 topoisomerase IIα (Affymetrix) in the absence or presence of increasing concentrations of compounds
593 under analysis. Assay mixtures contained supercoiled pBluescript DNA (0.3 μg), topoisomerase IIα (4
594 units) and the tested compounds (0–100 μM) in 20 μL of 1× TopoII reaction buffer (PN73592
595 Affymetrix, Inc.). Etoposide was used at 100 and 50 μM concentration as a control of the topo IIα
596 inhibitor. Reactions were incubated for 45 min at 37 °C and stopped by the addition of 2 μL of agarose
597 gel loading buffer. Samples were then subjected to electrophoresis and DNA bands were stained with
598 ethidium bromide as described above (0.5 μg mL−1) for 30 min and visualized by transillumination.
599
600 **Cathepsin B inhibition assay**
601 The colorimetric cathepsin B assay was performed as described by Casini et al.74 with a few
602 modifications. Briefly, the reaction mixture contained 100 mM sodium phosphate (pH 6.0), 1 mM
603 EDTA and 200 μM sodium N-carbobenzoxy- L-lysine p-nitrophenyl ester as a substrate. To make the
604 enzyme catalytically active before each experiment, the cysteine in the active site was reduced by
605 treatment with dithiothreitol (DTT). For this purpose, 5 mM DTT was added to the cathepsin B sample,
606 before dilution, and incubated 1 h at 30 °C. To test the inhibitory effect of the platinum compounds on
607 cathepsin B, activity measurements were performed in triplicate using fixed concentrations of the
608 enzyme (1 μM) and the substrate (200 μM). The platinum compounds were used at concentrations
609 ranging from 5 to 100 μM. Prior to the addition of the substrate, cathepsin B was incubated with the
610 different compounds at 25 °C for 2 h. The cysteine proteinase inhibitor E-64 was used as a positive
611 control of cathepsin B inhibition. Complete inhibition was achieved at 10 μM concentration of E-64.
612 Activity was measured over 90 s at 326 nm on a UV spectrophotometer.
613
614 **Cell cycle analysis**
615 Cell cycle was assessed by flow cytometry using a fluorescence activated cell sorter (FACS). For this
616 assay, 4 × 104 A-549 cells were seeded in 6 well plates with 2 mL of growth medium. After 24 h of
617 incubation, compounds 2b or 2c were added at their IC50 values 2.62 and 1.42 μM, respectively.
618 Following 72 h of incubation, cells were harvested by mild trypsinization, collected by centrifugation
619 and resuspended in Tris buffered saline solution (TBS) containing 50 mg mL−1 PI, 10 mg mL−1
620 DNase-free RNase and 0.1% Igepal CA-630. The cell suspension was incubated for 1 h at room
621 temperature to allow for the staining of the cells with PI, and afterwards FACS analysis was carried out

622 at 488 nm by employing a Gallios flow cytometer (Beckman Coulter). Data from 1 × 104 cells were
623 collected and analyzed using the FlowJo software.
624
625 **Apoptosis assay**
626 Apoptosis was assessed by evaluating the annexin-V binding to phosphatidylserine (PS), which is
627 externalized early in the apoptotic process. 4 × 104 A-549 cells per well were seeded in 6 well plates
628 with 2 mL of medium and treated as described for the cell cycle analysis assay. After cell collection and
629 centrifugation, the cells were resuspended in 95 μL binding buffer (10 mM HEPES/NaOH, pH 7.40, 140
630 mM NaCl, 2.5 mM CaCl2). 3 μL of the Annexin-V FITC conjugate (1 mg mL−1) were then added and
631 the suspension was incubated in the dark for 30 min, at room temperature. The cell suspension was
632 added to a vial containing 500 μL of binding buffer, stained with 20 μL of 1 mg mL−1 PI solution and
633 analyzed. Data from 1 × 104 cells were collected and analyzed using the FlowJo software.
634
635 **Determination of intracellular reactive oxygen species (ROS) levels**
636 4 × 104 A-549 cells per well were seeded in 6 well plates with 2 mL of growth medium and treated as
637 described for the cell cycle analysis assay. First, the cells were washed once with warm PBS, and
638 incubated with 5 μM 2′,7′-dichlorofluorescein diacetate (DCFH-DA, Invitrogen) in PBS supplemented
639 with 10 mM glucose and 2 mM glutamine for 30 min at 37 °C. Then, DCFH-DA solution in PBS was
640 replaced with the complete culture medium and the cells were incubated for another 30 min at 37 °C.
641 Finally, the cells were trypsinized and resuspended thoroughly in 0.4 mL of PBS containing DCFH-DA
642 (50 μM) and PI (20 μg mL−1).75 The intracellular internalized probe reacts with ROS and emits
643 fluorescence when excited at 492 nm. Emitted fluorescence was recorded by flow cytometry at 520 nm
644 using a Gallios flow cytometer (Beckman Coulter). The data of DCF fluorescence concentrations from 1
645 × 104 PI negative cells were collected and analysed using FlowJo software.
646 **Data analysis.** For each compound, a minimum of three independent experiments with triplicate values
647 were conducted to measure cell viability. A minimum of two independent experiments in triplicates
648 were performed for cell cycle analysis, assessment of apoptosis and ROS. Significant differences
649 compared to the control were assessed by Student's t-test where $p < 0.05$(*), $p < 0.01$(**) or $p <$
650 0.001(***) were taken into consideration. Data are given as the mean ± standard deviation (SD).
651

ACKNOWLEDGEMENTS

This work was supported by the Ministerio de Economia y Competitividad (Grants CTQ-2015-65040-P, CTQ-2015-65707- C2-1-P MINECO/FEDER, “Red de Excelencia MetalBio” CTQ 2015-71211-REDT, SAF2014-56059-R, and SAF2015-70270- REDT) and by the Generalitat de Catalunya (Grants 2014SGR-1017 and 2014SGR-00155, and Icrea Academia award 2015 granted to M. Cascante). The efficient contribution of Dr Francisco Cárdenas and Dra. A. Linares for NMR spectroscopy at the Scientific and Technological Centers of the University of Barcelona (CCiTUB) is gratefully acknowledged.

REFERENCES

1 T. C. Johnstone, K. Suntharalingam and S. J. Lippard, Chem. Rev., 2016, 116, 3436–3486.

2 U. Basu, B. Banik, R. Wen, R. K. Pathak and S. Dhar, Dalton Trans., 2016, 12992–13004.

3 D. Gibson, Dalton Trans., 2016, 12983–12991.

4 G. R. Kenny, S. W. Chuah, A. Crawford and C. J. Marmion, Eur. J. Inorg. Chem., 2017, 1596–1612.

5 D. A. K. Vezzu, Q. Lu, Y. H. Chen and S. Huo, J. Inorg. Biochem., 2014, 134, 49–56.

6 R. W.-Y. Sun, D.-L. Ma, E. L.-M. Wong and C.-M. Che, Dalton Trans., 2007, 4884–4892.

7 G. L. Edwards, D. S. Black, G. B. Deacon and L. P. Wakelin, Can. J. Chem., 2005, 83, 969–979.

8 G. L. Edwards, D. S. Black, G. B. Deacon and L. P. Wakelin, Can. J. Chem., 2005, 83, 980–989.

9 D. L. Ma and C. M. Che, Chem. – Eur. J., 2003, 9, 6133–6144.

10 P. K. M. Siu, D. L. Ma and C. M. Che, Chem. Commun., 2005, 1, 1025–1027.

11 R. W.-Y. Sun, A. L.-F. Chow, X.-H. Li, J. J. Yan, S. S.-Y. Chui and C.-M. Che, Chem. Sci., 2011, 2, 728.

12 H. L. Chan, D. L. Ma, M. Yang and C. M. Che, ChemBioChem, 2003, 4, 62–68.

13 J. Albert, R. Bosque, M. Crespo, J. Granell, C. López, R. Cortés, A. Gonzalez, J. Quirante, C. Calvis, R. Messeguer, L. Baldomà, J. Badia and M. Cascante, Bioorg. Med. Chem., 2013, 21, 4210–4217.

14 J. Albert, R. Bosque, M. Crespo, J. Granell, C. López, R. Martín, A. González, A. Jayaraman, J. Quirante, C. Calvis, J. Badía, L. Baldomà, M. Font-Bardia, M. Cascante and R. Messeguer, Dalton Trans., 2015, 44, 13602–13614.

15 R. Cortés, M. Crespo, L. Davin, R. Martín, J. Quirante, D. Ruiz, R. Messeguer, C. Calvis, L. Baldomà, J. Badia, M. Font-Bardía, T. Calvet and M. Cascante, Eur. J. Med. Chem., 2012, 54, 557–566.

16 A. Escolà, M. Crespo, J. Quirante, R. Cortés, A. Jayaraman, J. Badia, L. Baldoma, T. Calvet, M. Font-Bardia and M. Cascante, Organometallics, 2014, 33, 1740–1750.

17 A. Escolà, M. Crespo, C. López, J. Quirante, A. Jayaraman, I. H. Polat, J. Badía, L. Baldomà and M. Cascante, Bioorg. Med. Chem., 2016, 24, 5804–5815.

18 C. M. Anderson, M. W. Greenberg, L. Spano, L. Servatius and J. M. Tanski, J. Organomet. Chem., 2016, 819, 27–36.

19 C. M. Anderson, M. Crespo, M. C. Jennings, A. J. Lough, G. Ferguson and R. J. Puddephatt, Organometallics, 1991, 10, 2672–2679.

20 T. Calvet, M. Crespo, M. Font-Bardía, S. Jansat and M. Martínez, Organometallics, 2012, 31, 4367–4373.

21 M. Crespo, C. Grande and A. Klein, J. Chem. Soc., Dalton Trans., 1999, 1629–1638.

22 M. Crespo, C. Grande, A. Klein, M. Font-Bardía and X. Solans, J. Organomet. Chem., 1998, 563, 179–190.
23 J. A. Labinger, Organometallics, 2015, 34, 4784–4795.
24 L. Rendina and R. J. Puddephatt, Chem. Rev., 1997, 97, 1735–1754.
25 T. C. Johnstone, S. M. Alexander, J. J. Wilson and S. J. Lippard, Dalton Trans., 2015, 44, 119–129.
26 J. J. Wilson and S. J. Lippard, Chem. Rev., 2014, 114, 4470–4495.
27 Z. Xu, Z. Wang, S.-M. Yiu and G. Zhu, Dalton Trans., 2015, 44, 19918–19926.
28 J. Z. Zhang, P. Bonnitcha, E. Wexselblatt, A. V. Klein, Y. Najajreh, D. Gibson and T. W. Hambley, Chem. – Eur. J., 2013, 19, 1672–1676.
29 M. Ravera, E. Gabano, G. Pelosi, F. Fregonese, S. Tinello and D. Osella, Inorg. Chem., 2014, 53, 9326–9335.
30 M. Ravera, E. Gabano, M. Sardi, E. Monti, M. B. Gariboldi and D. Osella, Eur. J. Inorg. Chem., 2012, 21, 3441–3448.
31 T. C. Johnstone, J. J. Wilson and S. J. Lippard, Inorg. Chem., 2013, 52, 12234–12249.
32 M. Ghedini, D. Pucci, A. Crispini and G. Barberio, Organometallics, 1999, 18, 2116–2124.
33 C. M. Anderson, M. Crespo, M. Font-Bardia and X. Solans, J. Organomet. Chem., 2000, 604, 178–185.
34 C. M. Anderson, M. Crespo and F. D. Rochon, J. Organomet. Chem., 2001, 631, 164–174.
35 J. Rodríguez, J. Zafrilla, J. Albert, M. Crespo, J. Granell, T. Calvet and M. Font-Bardia, J. Organomet. Chem., 2009, 694, 2467–2475.
36 A. Capapé, M. Crespo, J. Granell, M. Font-Bardía and X. Solans, J. Organomet. Chem., 2005, 690, 4309–4318.
37 A. Gandioso, J. Valle-Sistac, L. Rodríguez, M. Crespo and M. Font-Bardía, Organometallics, 2014, 33, 561–570.
38 D. Musumeci, C. Platella, C. Riccardi, A. Merlino, T. Marzo, L. Massai, L. Messori and D. Montesarchio, Dalton Trans., 2016, 2, 8587–8600.
39 D. Cirri, S. Pillozzi, C. Gabbiani, J. Tricomi, G. Bartoli, M. Stefanini, E. Michelucci, A. Arcangeli, L. Messori and T. Marzo, Dalton Trans., 2017, 46, 3311–3317.
40 A. M. Basri, R. M. Lord, S. J. Allison, A. Rodríguez-Bárzano, S. J. Lucas, F. D. Janeway, H. J. Shepherd, C. M. Pask, R. M. Phillips and P. C. McGowan, Chem. – Eur. J., 2017, 23, 6341–6356.
41 T. A. K. Al-Allaf, L. J. Rashan, A. S. Abu-Surrah, R. Fawzi and M. Steimann, Transition Met. Chem., 1998, 23, 403–406.
42 S. M. Nabavizadeh, H. Amini, M. Rashidi, K. R. Pellarin, M. S. McCready, B. F. T. Cooper and R. J. Puddephatt, J. Organomet. Chem., 2012, 713, 60–67.
43 M. Crespo, M. Font-Bardia and M. Martínez, Dalton Trans., 2015, 19543–19552.

735 44 J. C. Wang, Nat. Rev. Mol. Cell Biol., 2002, 3, 430–440.
736 45 T. Li and L. F. Liu, Annu. Rev. Pharmacol. Toxicol., 2001, 53–77.
737 46 M. M. Heck and W. C. Earnshaw, J. Cell Biol., 1986, 103, 2569–2581.
738 47 C. Wang, J. Qin and S. Yuermao, Drug Discoveries Ther., 2012, 6, 230–237.
739 48 J. L. Nitiss, Biochim. Biophys. Acta, Gene Struct. Expression, 1998, 1400, 63–81.
740 49 D. S. Sappal, A. K. McClendon, J. A. Fleming, V. Thoroddsen, K. Connolly, C. Reimer, R. K.
741 Blackman, C. E. Bulawa, N. Osheroff, P. Charlton and L. A. Rudolph-Owen, Mol. Cancer
742 Ther., 2004, 3, 47–58.
743 50 P. Thapa, K. Y. Jun, T. M. Kadayat, C. Park, Z. Zheng, T. B. Thapa Magar, G. Bist, A. Shrestha,
744 Y. Na, Y. Kwon and E. S. Lee, Bioorg. Med. Chem., 2015, 23, 6454–6466.
745 51 J. Spencer, A. Casini, O. Zava, R. P. Rathnam, S. K. Velhanda, M. Pfeffer, S. K. Callear, M. B.
746 Hursthoused and P. J. Dyson, Dalton Trans., 2009, 10731–10735.
747 52 S. Diaz-Moralli, M. Tarrado-Castellarnau, A. Miranda and M. Cascante, Pharmacol. Ther.,
748 2013, 138, 255–271.
749 53 M. Zanuy, A. Ramos-Montoya, O. Villacañas, N. Canela, A. Miranda, E. Aguilar, N. Agell, O.
750 Bachs, J. Rubio- Martinez, M. D. Pujol, W.-N. P. Lee, S. Marin and M. Cascante,
751 Metabolomics, 2012, 8, 454–464.
752 54 M. Malumbres and M. Barbacid, Cancer Cell, 2006, 9, 2–4.
753 55 G. R. Bean, Y. T. Ganesan, Y. Dong, S. Takeda, H. Liu, P. M. Chan, Y. Huang, L. A. Chodosh,
754 G. P. Zambetti, J. J.-D. Hsieh and E. H.-Y. Cheng, Sci. Signaling, 2013, 6(268), ra20.
755 56 D. Hanahan and R. A. Weinberg, Cell, 2011, 144, 646–674.
756 57 B. Pucci, M. Kasten and A. Giordano, Neoplasia, 2000, 2, 291–299.
757 58 D. L. Bratton, E. Dreyer, J. M. Kailey, V. A. Fadok, K. L. Clay and P. M. Henson, J. Immunol.,
758 1992, 148, 514–523.
759 59 A. K. Hammill, J. W. Uhr and R. H. Scheuermann, Exp. Cell Res., 1999, 251, 16–21.
760 60 M. W. Lee, S. Ch. Parkb, Y. G. Yang, S. O. Yim, H. S. Chae, J.-H. Bach, H. J. Lee, K. Y. Kim,
761 W. B. Lee and S. S. Kim, FEBS Lett., 2002, 512, 313–318.
762 61 E. Giannoni, F. Buricchi, G. Raugei, G. Ramponi and P. Chiarugi, Mol. Cell Biol., 2005, 25,
763 6391–6403.
764 62 P. Gao, H. Zhang, R. Dinavahi, F. Li, Y. Xiang, V. Raman, Z. M. Bhujwalla, D. W. Felsher, L.
765 Cheng, J. Pevsner, L. A. Lee, G. L. Semenza and C. V. Dang, Cancer Cell, 2007, 12, 230–238.
766 63 A. Takahashi, N. Ohtani, K. Yamakoshi, S.-I. Iida, H. Tahara, K. Nakayama, K. I. Nakayama, T.
767 Ide, H. Saya and E. Hara, Nat. Cell Biol., 2006, 8, 1291–1297.
768 64 C. Garrido, L. Galluzzi, M. Brunet, P. E. Puig, C. Didelot and G. Kroemer, Cell Death Differ.,
769 2006, 13, 1423–1433.
770 65 A. Miyajima, J. Nakashima, K. Yoshioka, M. Tachibana, H. Tazaki and M. Murai, Br. J.
771 Cancer, 1997, 76, 206–210.

66 S. Dasari and P. B. Tchounwou, Eur. J. Pharmacol., 2014, 740, 364–378.
67 S. Göschl, P. V. Hristo, S. Theiner, M. A. Jakupec, M. Galanski and B. K. Keppler, J. Inorg. Biochem., 2016, 160, 264–274.
68 V. Pichler, S. Göschl, E. Schreiber-Brynzak, M. A. Jakupec, M. Galanski and B. K. Keppler, Metallomics, 2015, 7, 1078–1090.
69 G. S. Hill, M. J. Irwin, C. J. Levy, L. M. Rendina and R. J. Puddephatt, Inorg. Synth., 1998, 32, 149–153.
70 G. M. Sheldrick, Acta Crystallogr., Sect. C: Cryst. Struct. Commun., 2015, 71, 3–8.
71 T. Mosmann, J. Immunol. Methods, 1983, 65, 55–63.
72 C. Matito, F. Mastorakou, J. J. Centelles, J. L. Torres Simón and M. C. Serratosa, Eur. J. Nutr., 2003, 42, 43–49.
73 A. Abdullah, F. Huq, A. Chowdhury, H. Tayyem, P. Beale and K. Fisher, BMC Chem. Biol., 2006, 6, 3.
74 A. Casini, C. Gabbiani, F. Sorrentino, M. P. Rigobello, A. Bindoli, T. J. Geldbach, A. Marrone, N. Re, C. G. Hartinger, P. J. Dyson and L. Messori, J. Med. Chem., 2008, 51, 6773–6781.
75 M. Tarrado-Castellarnau, R. Cortés, M. Zanuy, J. Tarragó-Celada, I. H. Polat, R. Hill, T. W. M. Fan, W. Link and M. Cascante, Pharmacol. Res., 2015, 102, 218–234.

Legends to figures

Scheme 1 Possible pathways in the synthesis of cyclometallated platinum(IV) compounds. Method A: intramolecular C–Z oxidative addition observed for Z = Br or Cl. Method B: intermolecular YZ oxidative addition on a cyclometallated platinum(II) compound obtained for Z = H. L = labile ligand.

Scheme 2 Synthesis of cyclometallated platinum(II) compounds. (i) +cis-[PtCl2(dmso)2]/NaCH3COO (1 : 1 : 1) in refluxing methanol, 72 hours; (ii) +[Pt2(CH3)4{μ-S(CH3)2}2] (1 : 0.5) in refluxing toluene, 1 hour; (iii) +cis-[PtI2(dmso)2]/NaCH3COO (1 : 1 : 1) in refluxing methanol, 48 hours.

Figure. 1 Molecular structure of compound 1c showing 50% probability ellipsoids. Selected bond lengths (Å) and angles (°) with estimated standard deviations: Pt(1)–C(1): 2.002(3); Pt(1)–N(1): 2.031(2); Pt(1)–N(2): 2.199(2); Pt(1)–I(1): 2.5925(2); C(1)–Pt(1)–N(1): 80.64(10); N(1)–Pt(1)–N(2): 94.96(9); C(1)–Pt(1)–I(1): 92.91(7); N(2)–Pt(1)–I(1): 91.36(6).

Scheme 3 Oxidative addition reactions (including the numbering scheme used in the Experimental section and in Table 1).

Scheme 4 Possible isomers of compounds 2b and 3a leading to a mutually cis arrangement of Y and Z ligands.

Figure. 2 Molecular structure of compound 3b (molecule A) showing 50% probability ellipsoids. Selected bond lengths (Å) and angles (°) with estimated standard deviations: Pt(1A)–C(1A): 2.016(2); Pt(1A)–C(13A): 2.074(2); Pt(1)–N(1A): 2.1364(19); Pt(1A)–N(2A): 2.2672(19); Pt(1A)–I(1A): 2.6463(2); Pt(1A)–I(2A): 2.64964(18); C(1A)–Pt(1A)–C(13A): 94.80(9); C(1A)–Pt(1A)–N(1A): 79.76(81); C(13A)–Pt(1A)–N(2A): 91.01(8); N(1A)–Pt(1A)–N(2A): 94.44(7); C(1A)–Pt(1A)–I(1A): 84.01(6); C(13A)–Pt(1A)–I(1A): 88.52(7); N(1A)–Pt(1A)–I(1A): 90.10(5); N(2A)–Pt(1A)–I(1A): 96.70(5); C(13A)–Pt(1A)–I(2A): 91.57(7); C(1A)–Pt(1A)–I(2A): 86.14(6); N(1A)–Pt(1A)–I(2A): 88.88(5); N(2A)–Pt(1A)–I(2A): 93.17(5).

Figure. 3 Molecular structure of compound 3a' showing 50% probability ellipsoids. Selected bond lengths (Å) and angles (°) with estimated standard deviations: Pt(1)–C(1): 2.021(6); Pt(1)–Cl(1): 2.465(5); Pt(1)–N(1): 2.054(6); Pt(1)–N(2): 2.280(6); Pt(1)–I(1): 2.7568(5); Pt(1)–I(2): 2.6331(5); C(1)–Pt(1)–N(1): 80.5(3); N(1)–Pt(1)–N(2): 95.3(2); C(1)–Pt(1)–Cl(1): 83.3(2); C(1)–Pt(1)–Cl(1): 89.18(19); N(2)–Pt(1)–Cl(1): 94.83(18); C(1)–Pt(1)–I(2): 94.3(2); N(2)–Pt(1)–I(2): 89.83(15); Cl(1)–Pt(1)–I(2): 87.59(9); C(1)–Pt(1)–I(1): 88.88(19); N(1)–Pt(1)–I(1): 87.21(17); N(2)–Pt(1)–I(1): 92.75(16); I(2)–Pt(1)–I(1): 95.368(16).

827 **Scheme 5** Proposed species formed in solution (the charges of the ionic species are omitted).
828
829 **Figure. 4** Antiproliferative activity of platinum(II) compounds 1a–1c, platinum(IV) compounds 2a–2c
830 and 3a–3c, and cisplatin (IC50 μM) against A-549 lung, HCT-116 colon, MDA-MB-231 and MCF-7
831 breast human cancer cell lines.
832
833 **Figure 5**. Interaction of pBluescript SK+ plasmid DNA (0.8 μg) with increasing concentrations of
834 compounds 1a–1c, 2a–2c, 3a–3c, cisplatin and ethidium bromide (EB). Lane 1: DNA only. Lane 2: 2.5
835 μM. Lane 3: 5 μM. Lane 4: 10 μM. Lane 5: 25 μM. Lane 6: 50 μM. Lane 7: 100 μM. Lane 8: 200 μM. sc
836 = supercoiled closed circular DNA; oc = open circular DNA.
837
838 **Figure 6** Electrophoretograms of supercoiled pBluescript SK+ plasmid DNA incubated with increasing
839 concentrations of platinum(IV) compounds 2a–2c and 3a–3c in the absence (−AA) or presence (+AA) of
840 ascorbic acid (500 μM) for 24 h at 37 °C in 0.1× Tris-EDTA buffer (pH 7.8). Lane 1: (−) scDNA only.
841 Lane 2: 25 μM. Lane 3: 50 μM. Lane 4: 100 μM. Lane 5: 200 μM.
842
843 **Figure 7** Analysis of compounds 2a–2b and 3a–3c as putative topoisomerase IIα inhibitors. Supercoiled
844 pBluescript SK+ plasmid DNA was incubated with topoisomerase IIα (4 units) with increasing
845 concentrations of the compounds under study. Reactions containing etoposide (Et) are included as
846 examples of a topoisomerase IIα inhibitor. Lane 1: (−) scDNA only. Lane 2: 0 μM; Lane 3: 5 μM; Lane
847 4: 10 μM; Lane 5: 25 μM; Lane 6: 50 μM; Lane 7: 100 μM; Lane 8: 150 μM; Lane 9: 200 μM
848 compound. Except for line 1, all lines included topoisomerase IIα. The conversion of supercoiled DNA
849 to relaxed DNA was analyzed after 45 min incubation at 37 °C. sc = supercoiled closed circular DNA; R
850 = relaxed DNA.
851
852 **Figure 8** Cell cycle phase distribution at 72 h incubation with compounds 2b and 2c at their IC50
853 concentration in the A-549 lung adenocarcinoma cell line. Cells were stained with propidium iodide (PI)
854 and their DNA content was analyzed by flow cytometry.
855
856 **Figure 9** Percentage variations of alive, early apoptotic and late apoptotic/necrotic cell populations at 72
857 h incubation with compounds 2b and 2c at their IC50 concentration in the A-549 lung adenocarcinoma
858 cell line. Cells were stained with propidium iodide (PI) and FITC-annexin and were analyzed by flow
859 cytometry.
860
861 **Figure 10** ROS levels after 72 h incubation with compounds 2b and 2c at their IC50 concentration in the
862 A-549 lung adenocarcinoma cell line.
863

SCHEME 1

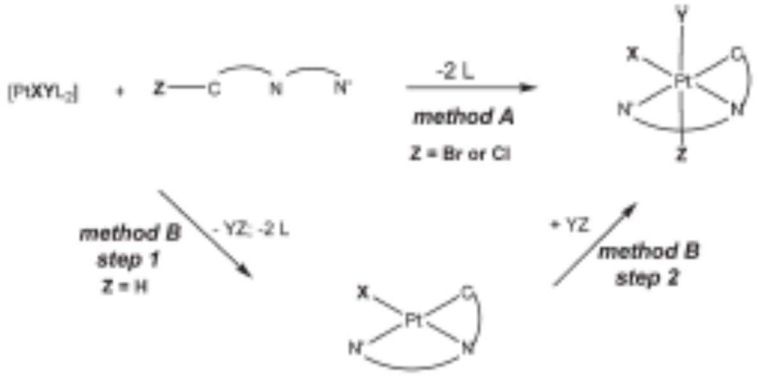
[PtXYL2]
Z
C
N
N'
-2 L
method A
Z = Br or Cl
Y
X
C
Pt
N'
N
Z
method B
step 1
Z = H
- YZ; -2 L
+ YZ
method B
step 2

SCHEME 2

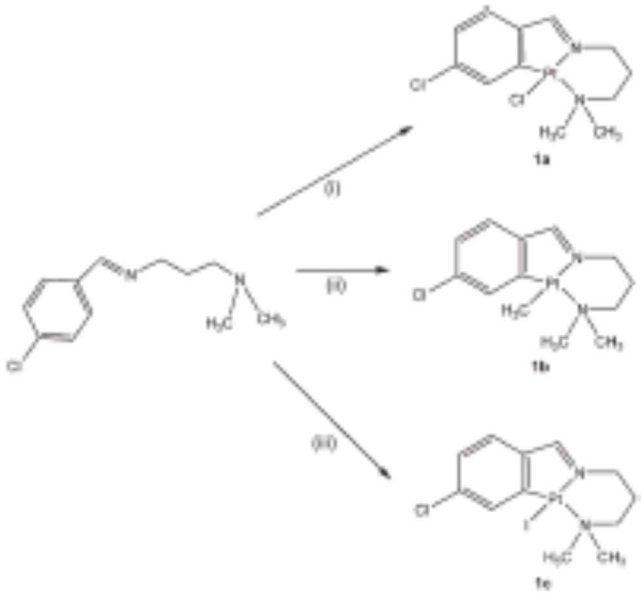

FIGURE 1

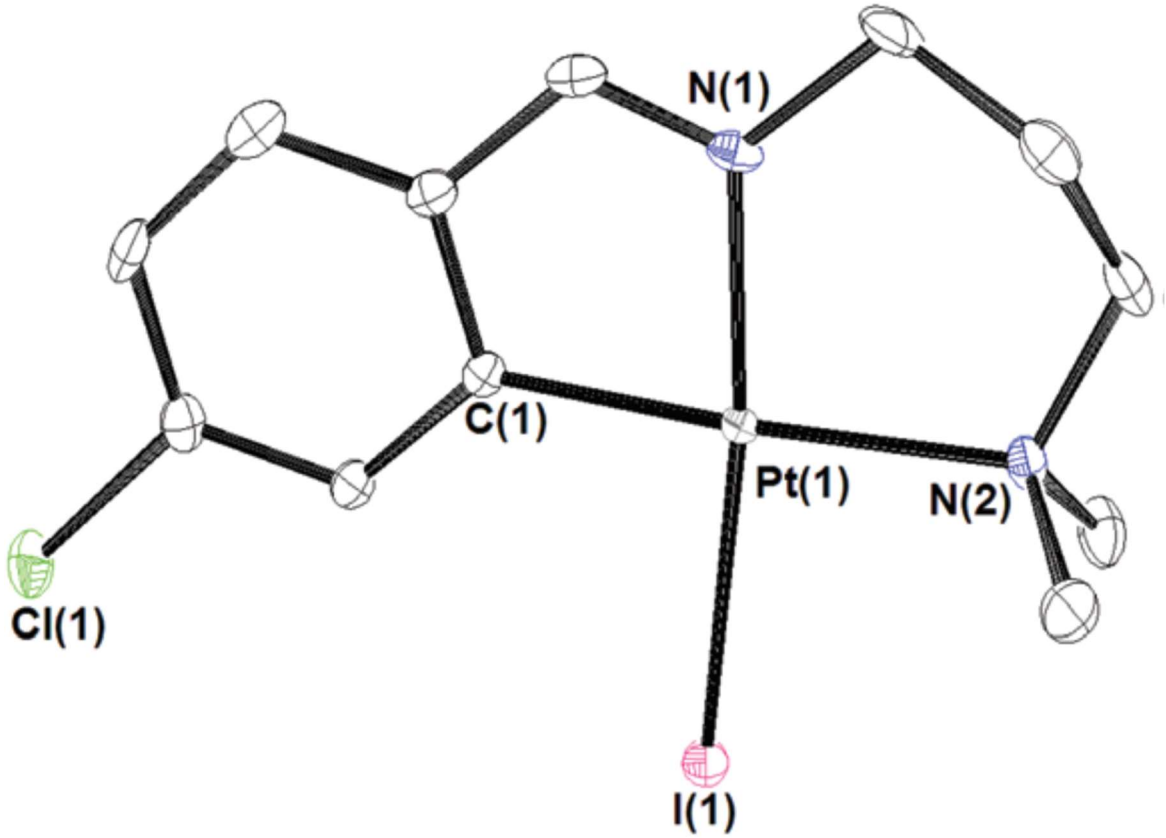

SCHEME 3

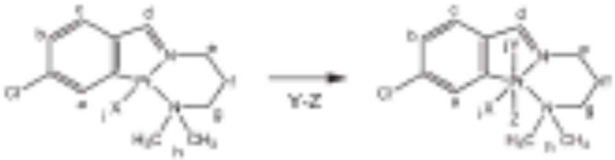

1a X = Cl
1b X = CH_3
1c X = I

2a X = Cl; Y = CH_3; Z = I
2b X = CH_3; Y = CH_3; Z = I
2c X = I; Y = CH_3; Z = I
3a X = Cl; Y = I; Z = I
3b X = CH_3; Y = I; Z = I
3c X = I; Y = I; Z = I

SCHEME 4

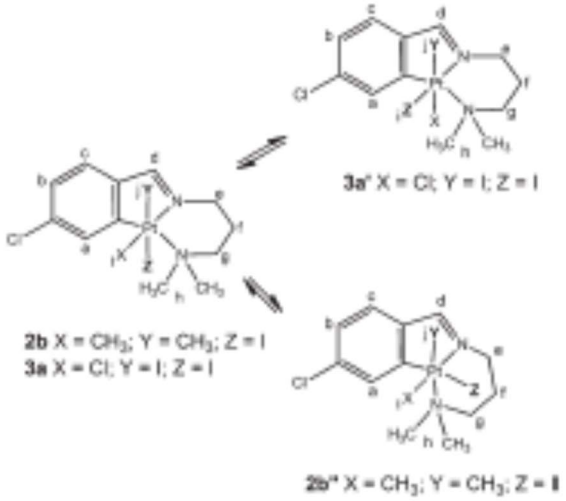

FIGURE 2

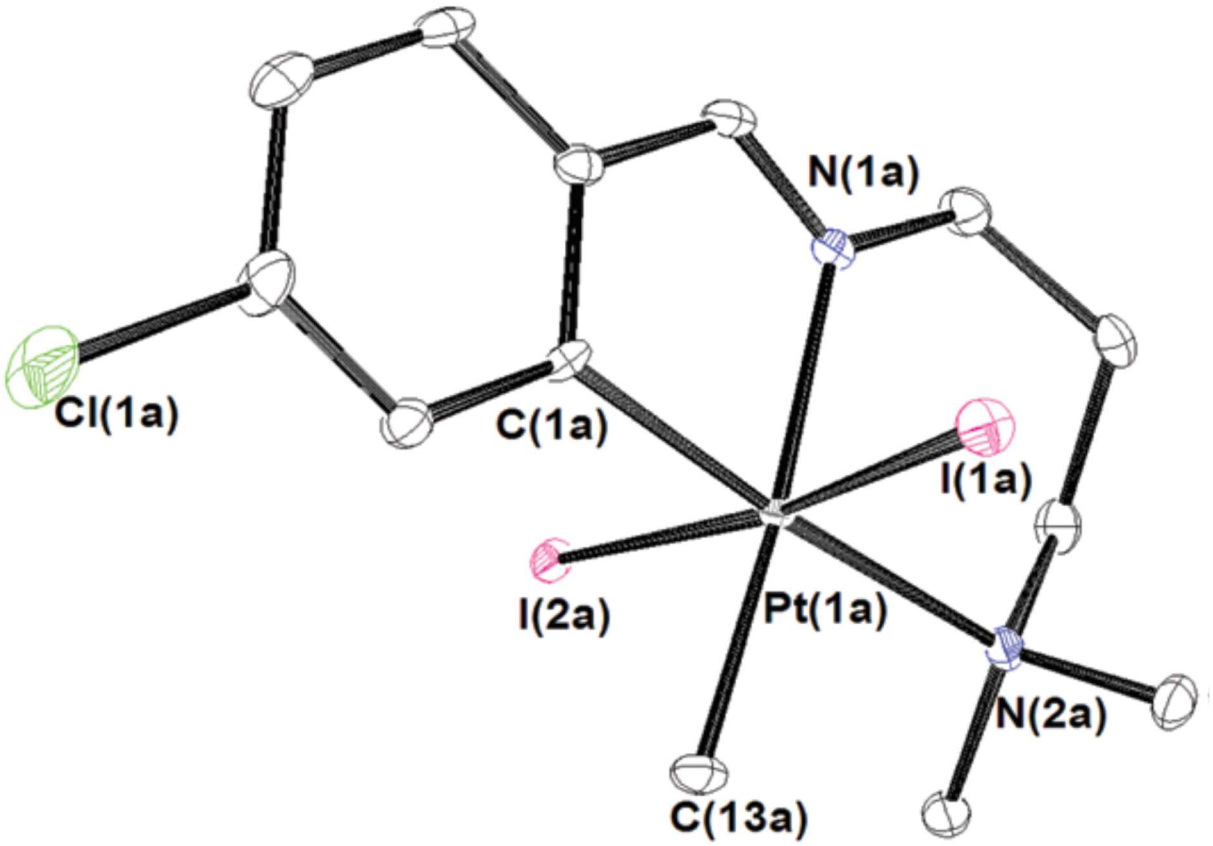

FIGURE 3

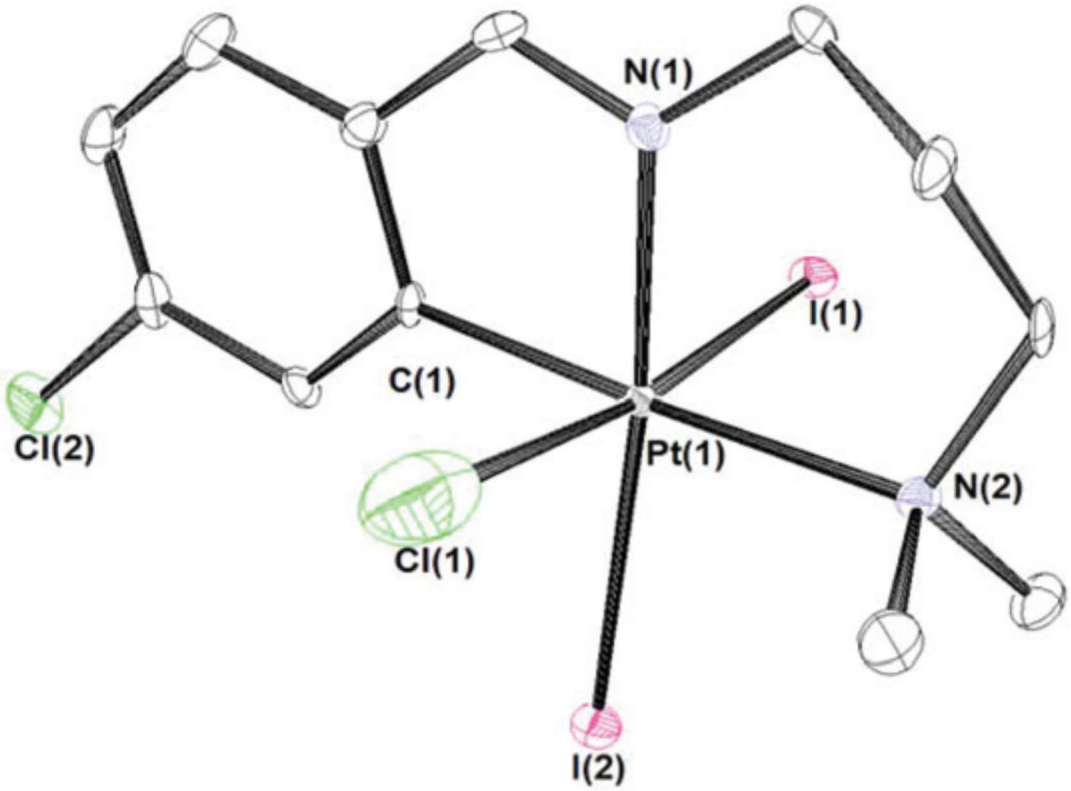

SCHEME 5

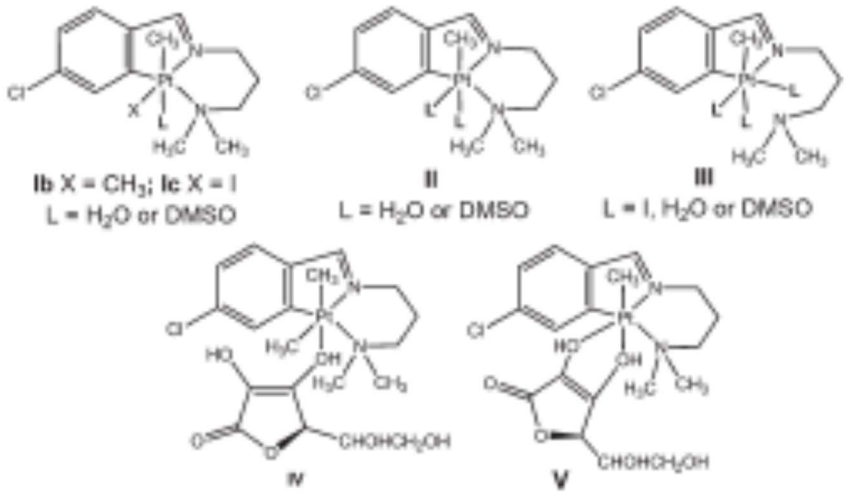

FIGURE 4

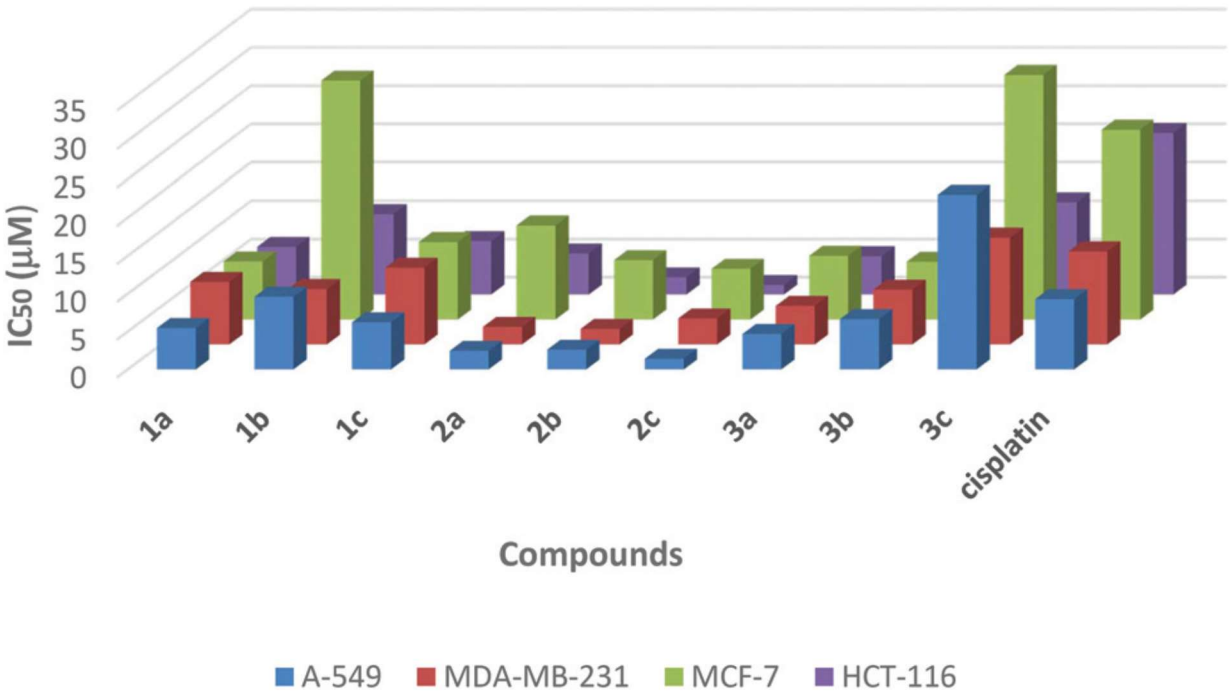
35
30
25
20
15
10
5
0
IC50 (µM)
1a
1b
1c
2a
2b
2c
3a
3b
3c
cisplatin
Compounds
A-549
MDA-MB-231
MCF-7
HCT-116

921 **FIGURE 5**

922

923

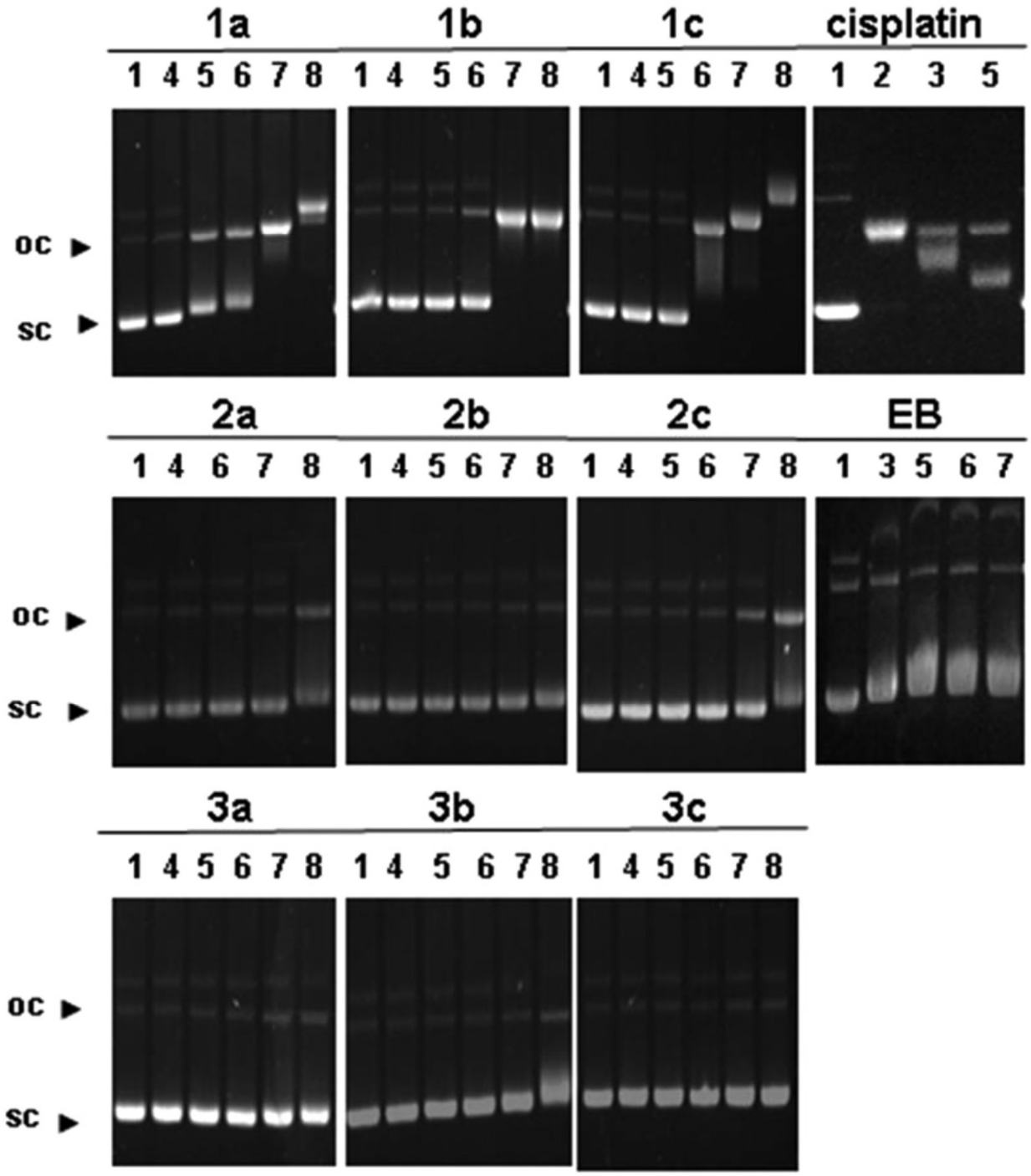

924

925

926 **FIGURE 6**

927

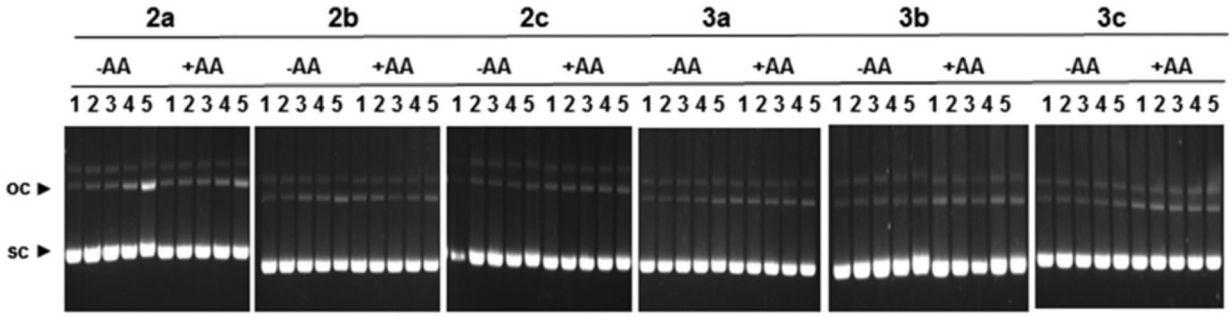

928

929

930 **FIGURE 7**

931
932

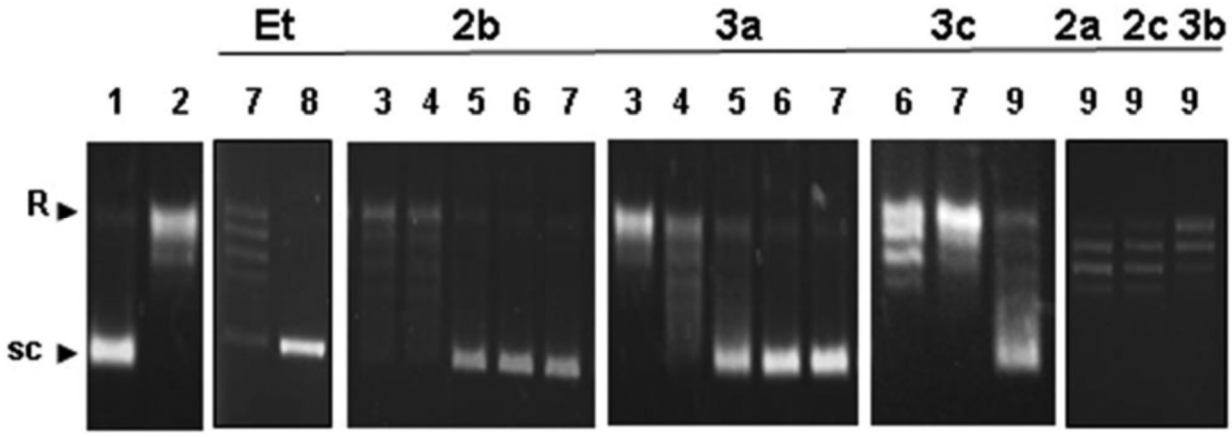

933
934
935

936 **FIGURE 8**

937

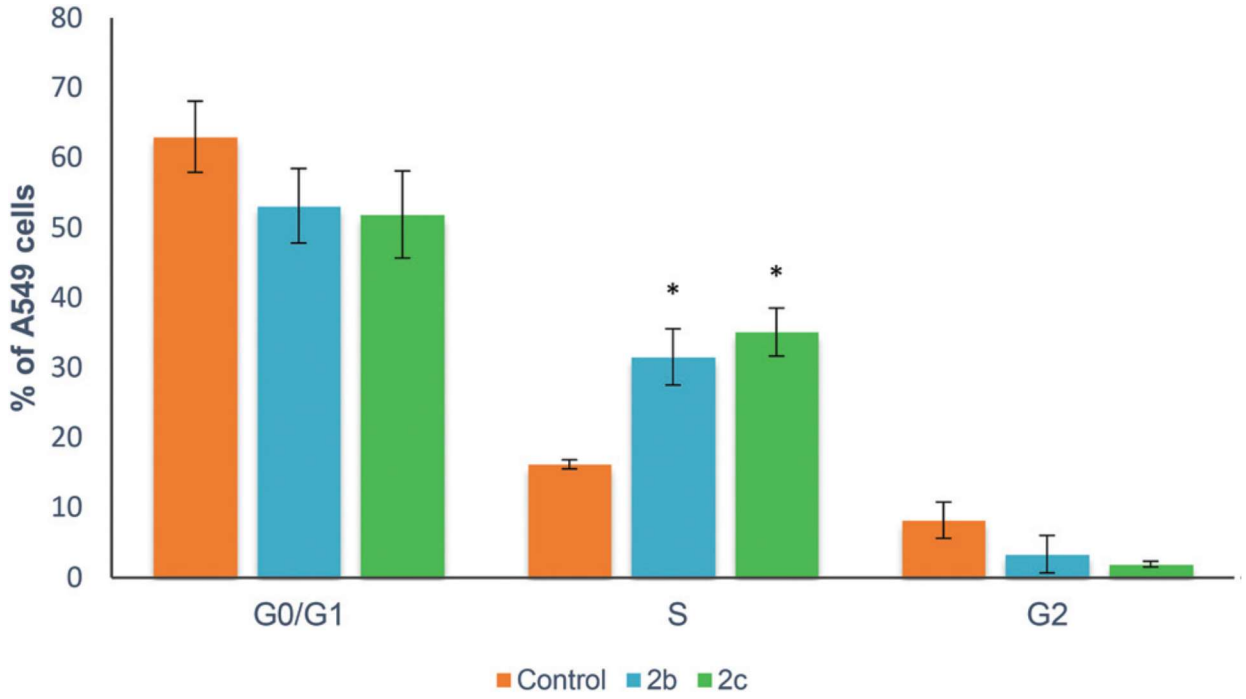

938
939

940 **FIGURE 9**

941
942
943

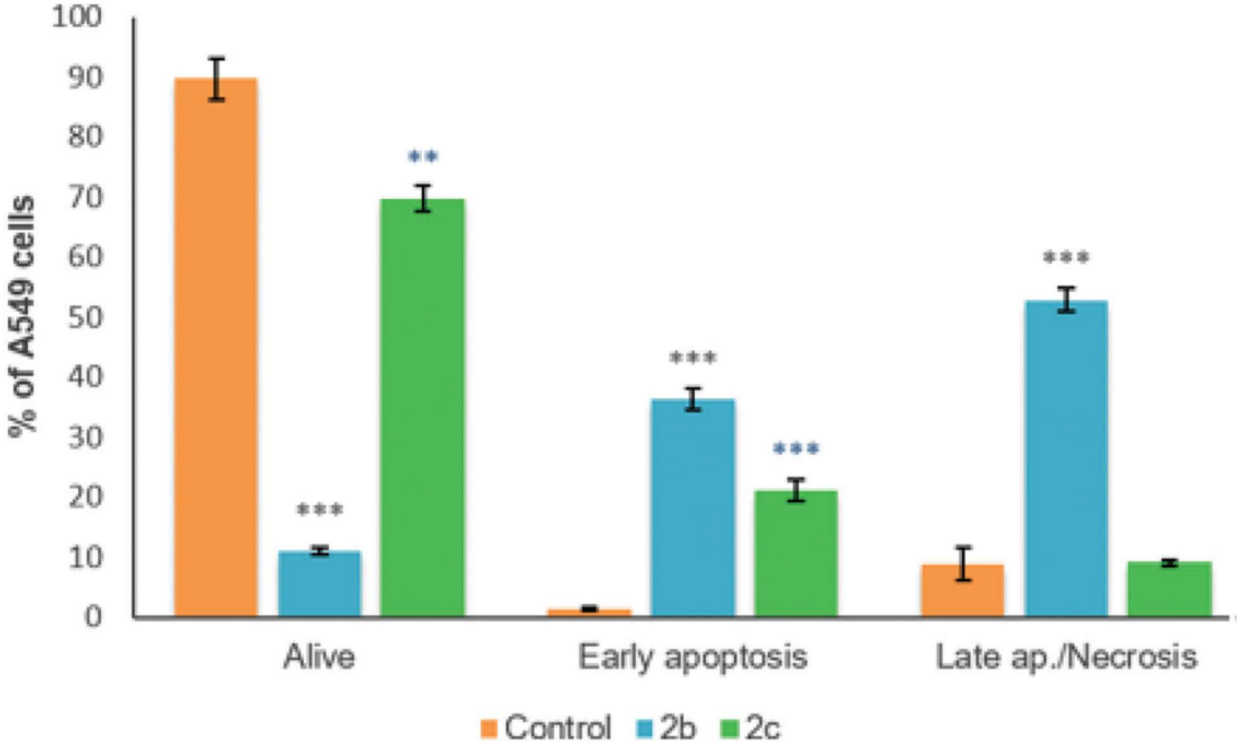

944
945

946 **FIGURE 10**

947

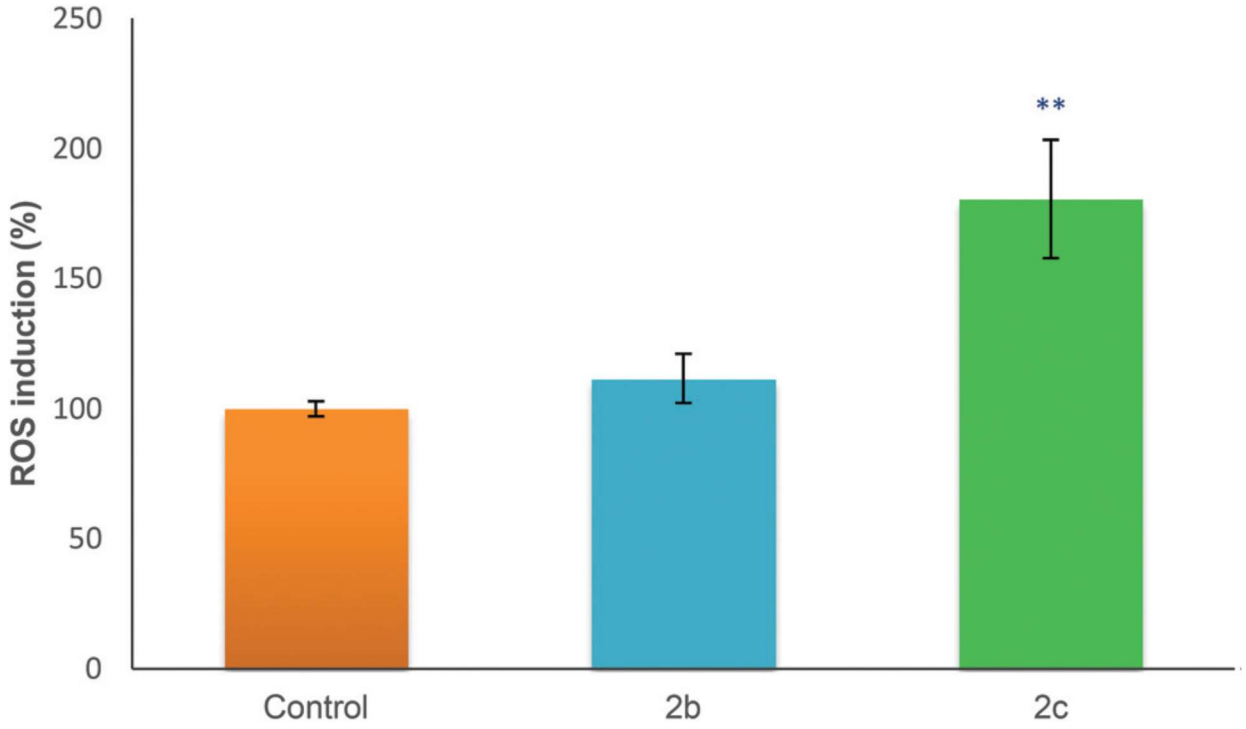

948
949

Table 1 Selected 1H NMR data of the studied compoundsa

	$\delta(H^a)$ [^3J(Pt–H)]	$\delta(H^b)$ [^3J(Pt–H)]	$\delta(CH_3)$ [^3J(Pt–H)]
1a[b]	8.29 [142.5]	2.81 [14.5]	—
1b	8.56 [59.6]	2.73 [23.6]	0.99 [80.8]
1c	8.42 [139.0]	3.01 [16.7]	—
2a[c]	8.77 [116.4]	3.43 [11.6]; 2.67 [15.2]	1.54 [64.8]
2b	8.39 [47.6]	3.19 [13.2]; 2.43 [17.2]	0.79 [69.2]; 1.38 [66.0]
2c	8.22 [104.0]	3.64 [13.9]; 2.72 [16.1]	1.71 [65.5]
3a	7.92 [95.2]	3.44 [14.8]	—
3b	8.16 [57.6]	3.11 [17.6]	2.21 [69.2]
3c	7.99 [88.0]	3.57 [16.8]	—

[a] In $CDCl_3$ unless otherwise stated, δ in ppm, J in Hz, labels as indicated in Scheme 3. [b] Values taken from ref. 36. [c] In acetone-d^6.

Table 2 Antiproliferative activity on A-549 lung, MDA-MB-231 and MCF-7 breast, and HCT-116 for the studied compounds and cisplatin

	IC_{50}[a] (μM)			
Compound	A-549	MDA-MB-231	MCF-7	HCT-116
1a	5.48 ± 3.49	8.30 ± 3.60	7.69 ± 0.750	6.29 ± 0.34
1b	9.62 ± 2.14	7.34 ± 0.59	31.26 ± 0.51	10.58 ± 0.22
1c	6.25 ± 2.66	10.18 ± 3.42	10.23 ± 0.48	7.05 ± 0.18
2a	2.46 ± 0.24	2.34 ± 0.33	12.39 ± 0.76	5.43 ± 0.13
2b	2.62 ± 0.27	2.06 ± 0.51	7.86 ± 0.72	2.28 ± 0.26
2c	1.42 ± 0.13	3.45 ± 1.55	6.72 ± 0.43	1.26 ± 0.18
3a	4.69 ± 3.61	5.11 ± 2.21	8.42 ± 0.41	5.06 ± 0.10
3b	6.67 ± 1.30	7.25 ± 0.23	7.65 ± 0.11	3.95 ± 1.62
3c	23.0 ± 2.98	14.10 ± 4.07	32.00 ± nd	12.11 ± 0.69
Cisplatin[b]	9.30 ± 3.00	12.31 ± 0.40	24.84 ± 0.40	21.10 ± 1.34

[a] Data are shown as the mean values of two experiments performed in triplicate with the corresponding standard deviations. [b] Cisplatin (*cis*-$[PtCl_2(NH_3)_2]$) is taken as the reference compound.

Table 3 Crystal data and structure refinement for 1c, 3b and 3a'

Compound	1c	3b	3a'
Formula	$C_{12}H_{16}ClIN_2Pt$	$C_{13}H_{19}ClI_2N_2Pt$	$C_{12}H_{16}Cl_2I_2N_2Pt$
Crystal size, mm	0.138 × 0.101 × 0.095	0.205 × 0.169 × 0.074	0.085 × 0.094 × 0.094
Fw	545.71	687.64	708.06
Temp., K	100(2)	100(2)	293(2)
Wavelength, Å	0.71073	0.71073	0.71073
Crystal system	Monoclinic	Triclinic	Orthorhombic
Space group	$P2_1/n$	$P1$	$Pna2_1$
a, Å	8.4203 (4)	8.5459 (4)	16.6399 (7)
b, Å	19.0185 (11)	14.1617 (7)	7.3056 (3)
c, Å	9.2913 (5)	14.8385 (7)	14.1494 (6)
α, °	90.0	80.425(2)	90.0
β, °	109.344 (2)	76.333 (2)	90.0
γ, °	90.0	86.586(2)	90.0
Volume, Å^3	1403.92 (13)	1720.28 (14)	1720.06 (12)
Z	4	4	4
D_{calc}, mg m^{-3}	2.582	2.655	2.734
Abs. coef., mm^{-1}	12.364	11.891	12.047
$F(000)$	1000	1248	1280
θ range for data collection, °	2.142 to 30.567	2.453 to 30.588	2.840 to 30.577
Reflns coll./independent	39 267/4288	77 498/10 509	80 936/5222
Data/restraint/parameters	4288/0/156	10 509/0/349	5222/1/175
GOF on F^2	1.125	1.130	1.124
Final R index ($I > 2\sigma(I)$)	R_1 = 0.0191, wR_2 = 0.0372	R_1 = 0.0170, wR_2 = 0.0345	R_1 = 0.0217, wR_2 = 0.0554
R index (all data)	R_1 = 0.0256, wR_2 = 0.0390	R_1 = 0.0204, wR_2 = 0.0353	R_1 = 0.0224, wR_2 = 0.0556
Peak and hole, e Å^{-3}	0.705 and −1.465	0.700 and −1.666	2.285 and −2.344
CCDC numbers	1565438	1565439	1565440